

**CONSTRUCTION OF *NptII*-*mtsfGFP* FUSION
GENE CONSTRUCT BY OVERLAP
EXTENSION PCR**

By

CHENG YANG YAN

A project report submitted to the Department of

Biological Science

Faculty of Science

Universiti Tunku Abdul Rahman

In partial fulfilment of the requirements for the degree of

Bachelor of Science (Honours) Biotechnology

OCTOBER 2025

Abstract

CONSTRUCTION OF *NptII*-*mtsfGFP* FUSION GENE CONSTRUCT BY OVERLAP EXTENSION PCR

CHENG YANG YAN

In plant transformation, the *Agrobacterium*-mediated system (AMT) is widely used due to deliver transgenes into multi-layered plant cells without causing damage. Previously, the GatewayTM-compatible binary vectors, pG103 and pG104 were built to enable convenient transgene insertion. For the selection of transformed cells, plasmid vectors pG103 and pG104 harbor the selectable markers *neomycin phosphotransferase* II (*NptII*) and mitochondrial recoded *neomycin phosphotransferase* II (*mtNptII*) genes, respectively, which confer resistance to aminoglycoside antibiotics for nuclear and mitochondrial transformation. To facilitate visualization of the protein expression of the gene of interest (GOI), a reporter gene is often translationally fused it. The green fluorescent protein (*GFP*) gene is widely used as a reporter gene. This project used mitochondrial recoded superfolder GFP (*mtsfGFP*) gene, which encode the same superfolder GFP protein, is designed for expression in either the host's nucleus and mitochondria. This project aimed to fuse the *NptII* and *mtNptII* with *mtsfGFP* using overlap extension PCR (OE-PCR). A 3-step OE-PCR approach using megaprimers was employed. However, due to the formation of secondary structures of the megaprimer during the PCR reaction, non-specific amplicons

were generated. To eliminate these non-specific amplicons and obtain the desired amplicons, parameters such as primer and template DNA concentrations, number of thermal cycles, and annealing temperature, were performed for each step of the OE-PCR. Consequently, amplicons carrying the *NptII-^{mt}sfGFP* and *^{mt}NptII-^{mt}sfGFP* fusion genes were successfully generated. In the future, these amplicons will be cloned into the *Agrobacterium* binary vectors for host transformation. They will facilitate qualitative and quantitative analysis of transgenes in the host's nucleus and mitochondria.

ACKNOWLEDGEMENTS

First, I would like to express my special thanks of gratitude to my supervisor, Prof. Dr. Wong Hann Ling. Without his support, priceless recommendations, and guidance throughout my final year project, I would not have been able to complete it. Prof. Wong is professional, patient, and kind; he always helped me solve problems whenever I faced difficulties. I am also grateful to my postgraduate seniors, Mrs. Yap Kiao Huio and Mr. Jordan Ooi, as well as my PhD senior, Mr. Toh Wai Keat, for everything. They assisted me whenever I encountered challenges in my project, discussed solutions with me, and supported me during my benchwork. I would like to thank my parents, sister, friends, Lim Wei, and Jeon Won Woo. Lastly, I want to thank my benchmates, Victoria Law and Lam Yee Ling.

APPROVAL SHEET

This final year project report entitled “**CONSTRUCTION OF *NptII-m⁺sfGFP*** **FUSION GENE CONSTRUCT BY OVERLAP EXTENSION PCR**” was prepared by CHENG YANG YAN and submitted as partial fulfilment of the requirements for the degree of Bachelor of Science (Honours) Biotechnology at Universiti Tunku Abdul Rahman.

Approved by:



03.09.2025

Date: _____

PROF. DR. WONG HANN LING

Supervisor

Department of Biological Science

Faculty of Science

Universiti Tunku Abdul Rahman

DECLARATION

I hereby declare that the project report is based on my original work except for quotation and citations, which have been duly acknowledged. I also declare that it has not been previously or concurrently submitted for any other degree at Universiti Tunku Abdul Rahman (UTAR) or other institutions.

Student's signature

TABLE OF CONTENT

	Page
ABSTRACT	ii
ACKNOWLEDGEMENTS	iv
APPROVAL SHEET	v
DECLARATION	vi
TABLE OF CONTENT	vii
LIST OF TABLES	xii
LIST OF FIGURES	xiv
LIST OF ABBREVIATIONS	xv
 CHAPTER	
1.0 INTRODUCTION	1
1.1 Plant transformation	2
1.2 <i>Neomycin phosphotransferase</i> II (<i>NptII</i>) and mitochondrial <i>neomycin phosphotransferase</i> II (^{mt} <i>NptII</i>): Selectable markers	3
1.3 Mitochondrial superfolder green fluorescent protein (^{mt} <i>sfGFP</i>): A reliable reporter gene	4
1.4 Overlap extension PCR: An effective fusion method	5
1.5 Dual-function plasmid: The fusion of the selectable marker and reporter gene	6
1.6 Objectives of this study	
2.0 LITERATURE REVIEW	7
2.1 <i>Agrobacterium</i> -mediated transformation (AMT)	7
2.1.1 Advances in AMT Methodology	8
2.1.2 Binary vector system	9
2.1.3 Engineered <i>Agrobacterium</i> -mediated	11

	transformation	
2.2	Gateway cloning	12
2.2.1	Principle of Gateway cloning	13
2.2.2	Entry vector (pENTR)	15
2.3	<i>Neomycin phosphotransferase II (NptII): A Reliable Selectable Marker</i>	16
2.1.3	<i>Mitochondrial NptII (^{mt}NptII): A modified version from NptII</i>	17
2.4	Green fluorescent protein (<i>GFP</i>)	18
2.4.1	GFP's three-dimensional structure	19
2.4.2	Mechanism of the chromophore	19
2.5	Mitochondrial superfolder green fluorescent protein (<i>sfGFP</i>)	21
3.0	METHODOLOGY	23
3.1	Experimental workflow of the project	23
3.2	Preparation of buffer, reagents and apparatus	24
3.2.1	Preparation of 5 x Tris/Borate/EDTA (TBE) buffer	24
3.2.2	Preparation of 3 M sodium acetate (NaOAc) solution	25
3.3	Agarose gel electrophoresis	25
3.4	Purification of PCR fragment using EZ-10 Spin Column DNA Gel Extraction Kit	26
3.5	Construction of <i>NptII/^{mt}NptII-sfGFP</i> fusion gene	28
3.5.1	Graphical overview of fusion gene construction	28
3.5.2	Megaprimer design	29
3.5.3	Single-primer amplification test with DNA template	31

	3.5.4 PCR amplification of <i>NptII</i> , <i>^{mt}NptII</i> , and <i>^{mt}sfGFP</i> gene fragment	33
	3.5.5 Overlap extension PCR for <i>NptII/^{mt}NptII-</i> , <i>^{mt}sfGFP</i> fusion gene fragment	35
	3.5.6 Final <i>NptII/^{mt}NptII-</i> , <i>^{mt}sfGFP</i> fusion gene PCR amplification	38
	3.6 Purification of <i>NptII</i> - <i>mtsfGFP</i> fusion gene fragment	40
	3.7 Purification of <i>mtNptII</i> - <i>mtsfGFP</i> fusion gene fragment	40
	3.7.1 Low-melting agarose gel electrophoresis	40
	3.7.2 Ethanol precipitation for gel purification	41
	3.8 DNA sequencing	42
4.0	RESULT	43
	4.1 Construction of <i>NptII/^{mt}NptII-</i> <i>^{mt}sfGFP</i> fusion gene	43
	4.1.1 Megaprimer Design	43
	4.2 Single-primer amplification test with DNA template	46
	4.3 PCR amplification of gene fragment	47
	4.3.1 <i>NptII</i> , <i>^{mt}NptII</i> , and <i>^{mt}sfGFP</i> gene fragments	47
	4.2.2 Result of agarose gel electrophoresis	48
	4.2.3 Quantification of purified product	49
	4.4 Overlap extension PCR for construct <i>NptII-</i> <i>^{mt}sfGFP</i> and <i>^{mt}NptII-</i> <i>^{mt}sfGFP</i> fusion gene	50
	4.4.1 <i>NptII-</i> <i>^{mt}sfGFP</i> and <i>^{mt}NptII-</i> <i>^{mt}sfGFP</i> fusion gene	50
	4.4.2 Result of agarose gel electrophoresis	51
	4.4.3 Quantification of purified product	52
	4.5 Verification of the fusion gene product by DNA sequencing	53

5.0	DISCUSSION	54
5.1	Justification for using overlap extension PCR in generate the fusion gene construction	54
5.2	Megaprimer design	56
5.3	Challenges in single-primer testing	57
5.4	Amplification of the target gene fragments	59
5.5	Overlap extension PCR	60
5.6	Purification of <i>NptII^{-mt}sfGFP</i> and <i>^{mt}NptII^{-mt}sfGFP</i> fusion genes products	62
5.7	DNA sequencing	63
5.8	The fusion pf selectable marker and reporter gene	64
5.8.1	Advantages of selectable marker and reporter gene	64
5.8.2	Disadvantages of selectable marker and reporter gene	65
5.9	Trouble shooting	66
5.10	Further studies	67
6.0	CONCLUSION	69
REFERE- NCES		71
Appendix A	The list of chemicals, reagents, and kits used in this final year project with their corresponding manufactures.	79
Appendix B	The plasmid's map for each DNA template.	81
Appendix C	Alignment of <i>NptII^{-mt}sfGFP</i> fusion gene product.	82
Appendix D	Genetic map for <i>NptII^{-mt}sfGFP</i> fusion gene product.	83
Appendix E	Alignment of <i>NptII^{-mt}sfGFP</i> fusion gene product.	84
Appendix F	Genetic map for <i>^{mt}NptII^{-mt}sfGFP</i> fusion gene product	87
Appendix G	Alignment of <i>NptII^{-mt}sfGFP</i> fusion gene product	89

LIST OF TABLES

Table	Page
3.1 Nucleotide sequence of primers used to amplify the <i>NptII</i> gene fragment from the pENTR-P _{TEF1} - <i>NptII</i> plasmid.	30
3.2 Nucleotide sequences of primers used to amplify <i>mtNptII</i> gene fragments from the pENTR-P _{Cox1} - <i>mtNptII</i> plasmid.	30
3.3 Nucleotide sequences of primers used to amplify the <i>mtsfGFP</i> gene fragment from pENTR-P _{Cox2} - <i>mtsfGFP</i> plasmid	30
3.4 PCR master mix and reaction components with their corresponding volumes.	31
3.5 PCR thermocycling parameters for <i>mtNptII</i> and <i>mtsfGFP</i> single primer testing with the extracted pENTR-P _{Cox1} - <i>mtNptII</i> and pENTR-P _{Cox2} - <i>mtsfGFP</i> plasmids, respectively	32
3.6 PCR thermocycling parameters for <i>NptII</i> single-primer amplification with the extracted pENTR-p _{TEF1} - <i>NptII</i> plasmid.	32
3.7 PCR master mix and reaction components with their corresponding volumes.	33
3.8 PCR thermocycling parameters for amplifying <i>NptII</i> with the extracted pENTR-P _{TEF1} - <i>NptII</i> plasmid	34
3.9 PCR thermocycling parameters for amplifying <i>mtNptII/mtsfGFP</i> with the extracted pENTR-P _{Cox1} - <i>mtNptII</i> /pENTR-P _{Cox2} - <i>mtsfGFP</i> plasmid.	34
3.10 PCR master mix and reaction components with their corresponding volumes for the <i>NptII-mtsfGFP</i> fusion gene.	36
3.11 PCR master mix and reaction components with their corresponding volumes for <i>mtNptII-mtsfGFP</i> fusion gene.	37
3.12 PCR thermocycling parameters for constructing the <i>NptII/mtNptII-mtsfGFP</i> fusion gene.	37
3.13 Nucleotide sequences of the outer primers used to amplify the <i>NptII/mtNptII-mtsfGFP</i> fusion gene fragment.	38

3.14	PCR mixtures and primers added with their corresponding volumes	38
3.15	PCR thermocycling parameters for amplifying the <i>NptII</i> - <i>mtsfGFP</i> fusion gene.	39
3.16	PCR thermocycling parameters for amplifying the <i>mtNptII</i> - <i>mtsfGFP</i> fusion gene.	39
4.1	Concentrations and purities of purified <i>NptII</i> , <i>mtNptII</i> and <i>mtsfGFP</i> fragments.	49
4.2	Concentrations and purities of purified <i>NptII</i> - <i>mtsfGFP</i> and <i>mtNptII</i> - <i>mtsfGFP</i> fusion genes.	52

LIST OF FIGURES

Figure		Page
2.1	Schematic showing the flowchart of the Gateway cloning reaction.	14
2.2	sfGFP's spatial structure.	22
3.1	Experimental workflow of construct <i>NptII</i> - <i>mt</i> sfGFP fusion gene.	23
3.2	Experimental workflow of construct <i>mt</i> <i>NptII</i> - <i>mt</i> sfGFP fusion gene.	24
3.3	Graphical overview of constructing the <i>NptII</i> / <i>mt</i> <i>NptII</i> <i>mt</i> sfGFP fusion gene by overlap extension PCR.	28
3.4	Schematic diagram showing megaprimer design to construct the <i>NptII</i> / <i>mt</i> <i>NptII</i> - <i>mt</i> sfGFP fusion gene.	29
4.1	Schematic showing the sequence of the <i>NptII</i> / <i>mt</i> <i>NptII</i> - <i>mt</i> sfGFP fusion gene.	43
4.2	Analysis of megaprimer secondary structure using an Oligonucleotide Properties Calculator.	44
4.3	Inverted 1.2% agarose gel image from the single-primer amplification test with the corresponding DNA template.	46
4.4	Schematic showing the sequence of the <i>NptII</i> , <i>mt</i> <i>NptII</i> , and <i>mt</i> sfGFP gene fragments with their primers.	47
4.5	PCR amplification for <i>NptII</i> , <i>mt</i> <i>NptII</i> , and <i>mt</i> sfGFP gene fragments was electrophoresed on a 1.2% (w/v) agarose gel.	48
4.6	Schematic showing the sequence of the construction of the <i>NptII</i> - <i>mt</i> sfGFP and <i>mt</i> <i>NptII</i> - <i>mt</i> sfGFP fusion genes.	50
4.7	Overlap extension PCR for <i>NptII</i> - <i>mt</i> sfGFP and <i>mt</i> <i>NptII</i> - <i>mt</i> sfGFP fusion genes electrophoresed on 0.8% (w/v) agarose gel.	51
Appendix A	The list of chemicals, reagents, and kits used in this final year project with their corresponding manufactures.	79

Appendix B	The plasmid's map for each DNA template.	81
Appendix C	Alignment of <i>NptII</i> - <i>mtsfGFP</i> fusion gene product.	82
Appendix D	Genetic map for <i>NptII</i> - <i>mtsfGFP</i> fusion gene product.	83
Appendix E	Alignment of <i>NptII</i> - <i>mtsfGFP</i> fusion gene product.	84
Appendix F	Genetic map for <i>mtNptII</i> - <i>mtsfGFP</i> fusion gene product	87
Appendix G	Alignment of <i>NptII</i> - <i>mtsfGFP</i> fusion gene product	89

LIST OF ABBREVIATIONS

AMT	<i>Agrobacterium</i> -mediated system
<i>A. tumefaciens</i>	<i>Agrobacterium tumefaciens</i>
bp	Base pair
°C	Degree Celsius
COX1	Cytochrome c oxidase subunit 1
COX2	Cytochrome c oxidase subunit 2
dH ₂ O	Distilled water
DMSO	Dimethyl sulfoxide
<i>E. coli</i>	<i>Escherichia coli</i>
EDTA	Ethylenediaminetetraacetic acid
EtOH	Ethyl alcohol
× <i>g</i>	Times gravity
G418	Geneticin
<i>GFP</i>	Green fluorescent protein
Gly67	Glycine in 67 th position
GOI	Gene of interest
h	Hour
HR	Homologous recombination
kb	Kilobase pair
kDNA	Kinetoplast DNA
L	Litre
min	Minute
mL	Millilitre
µg	Microgram

μL	Microlitre
μM	Micromolar
mtDNA	Mitochondrial genome
<i>mtNptII</i>	Mitochondrial recoded <i>neomycin phosphotransferase</i> II
MTS	Mitochondrial targeting sequences
<i>mtsfGFP</i>	Mitochondrial recoded superfolder GFP
<i>mtsfGFP(mtNptII)</i>	Mitochondrial recoded superfolder GFP overlapping with Mitochondrial recoded <i>neomycin phosphotransferase</i> II
<i>mtsfGFP(NptII)</i>	Mitochondrial recoded superfolder GFP overlapping with <i>neomycin phosphotransferase</i> II
NaOH	Sodium Hydroxide
NaOAc	Sodium acetate
nDNA	Nuclear genome
<i>Neo</i>	Neomycin
nm	Nanometers
<i>NptII</i>	<i>Neomycin phosphotransferase</i> II
OE-PCR	Overlap extension PCR
PCI	Phenol-chloroform-isoamyl alcohol
PCR	Polymerase Chain Reaction
pDEST	Destination vector
pDONR	Donor vector

pENTR	Entry plasmid
pEXPR	Expression vector
rRNA	Ribosomal RNA
rpm	Revolutions per minute
s	Second
Ser65	Serine in 65 th position
<i>sfGFP</i>	Superfolder green fluorescent protein
TBE	Tris/Borate/EDTA
T-DNA	Transferred DNA
<i>TEF1</i>	<i>Translation elongation factor 1α</i>
Ti	Tumor-inducing
T _m	Melting temperature
tRNAs	Transfer ribonucleic acid
Tyr66	Tyrosine in 66 th position
UV	Ultraviolet
V	Volt
<i>vir</i>	Virulence

CHAPTER 1

INTRODUCTION

1.1 Plant transformation

In the field of plant biotechnology, plant transformation is a fundamental tool, allowing the introduction of foreign genes into plant genomes. This technique contributes to the agricultural field by improving plant traits, such as productivity, resistance to trash environments, and increasing nutritional value. To generate the transformed plant, the foreign gene is delivered, integrated, and expressed into the plant cells through different methods, such as *Agrobacterium*-mediated transformation, biolistics, electroporation, and microinjection. (Kumar and Ling, 2021; Law, Miyamoto and Numata, 2023). *Agrobacterium*-mediated transformation is the most common method for plant genetic engineering because it efficiently delivers DNA through the multilayered plant cell wall without causing significant damage. However, the efficiency of forming transformed cells is low, even in the most successful transfer system (Hwang, Yu and Lai, 2017). Therefore, the selective methods are vital to identify and select the transformed cell in the plant transformation process. One of the most significant selective methods to distinguish transformed from non-transformed cells under selective conditions is the selectable marker.

1.2 *Neomycin phosphotransferase II (NptII)* and mitochondrial *neomycin phosphotransferase II* (^{mt}*NptII*): Selectable markers

Selectable marker genes are essential tools for plant transformation and are typically involved in the same DNA construct as the gene of interest. Most commonly, these genes make transformed cells resistant to antibiotics and survive when exposed to a selective medium. The *NptII* gene serves as an antibiotic selectable marker, and is usually inserted into plasmid vectors used for genetic transformation. *Neomycin phosphotransferase II (NptII)*, also known as *aminoglycoside 3'-phosphotransferase II*, is a type of transferase isolated from transposon Tn5 found in *Escherichia coli* (*E. coli*), which encodes *NptII* (E.C. 2.7.1.95). *NptII* can phosphorylate aminoglycoside antibiotics to inactivate their function. Under the selection medium, the transformed colonies can survive and grow due to resistance to antibiotics (Das et al., 2020).

The ^{mt}*NptII* gene is a modified version of the *NptII* gene, recoded according to the yeast mitochondrial genetic code. When expressed from the yeast mitochondrial genome, it produces the same protein as the ordinary *NptII* gene and confers resistance to aminoglycoside antibiotics, just like the nuclear-encoded version (Yap, 2025).

1.3 Mitochondrial superfolder green fluorescent protein (*mtsfGFP*): A reliable reporter gene

In plant transformation, the reporter gene is co-introduced with the gene of interest to provide a measurable or visual signal that proves the successful gene transfer and expression in the plant cell. The green fluorescent protein (*GFP*) is a widely used reporter gene. *GFP* was originally derived from the jellyfish (*Aequorea victoria*). Subsequently, a similar green fluorescent protein (*GFP*) was discovered in the sea pansies, *Renilla reniformis* (Soboleski, Oaks and Halford, 2005). Unlike most fluorescent proteins, which require an external cofactor for visualization, *GFP* can be detected directly by fluorescence microscopy without an exogenous substrate. It consists of 238 amino acids; and cyclization of three residues (positions 65-67) forms a unique chromophore. When exposed to blue or ultraviolet light, the chromophore will be triggered and emit green fluorescence (Pedelacq and Cabantous, 2019).

However, there are some limitations to traditional *GFP*, such as poor folding efficiency or weaker fluorescence in challenging cellular environments, which affect fluorescence intensity. Hence, superfolder green fluorescent protein (*sfGFP*) was used in this project because of its folding kinetics and stability. *sfGFP* is an engineered variant of *GFP* that contains multiple mutations, has a higher folding yield, and causes brighter and more stable fluorescence. The fluorescence capability of *sfGFP* was stable even after fusion with other proteins or misfolding. These features allow *sfGFP* to function in different

biological applications, such as a reporter for protein localization or protein-protein interaction detection. Mitochondrial superfolder green fluorescent protein (*^{mt}sfGFP*) is an engineered variant of *sfGFP* expressed in the nucleus and mitochondria. A few nucleotide sequences in *sfGFP* were modified to remove the stop codon and enable protein synthesis when integrated with the mitochondrial genome (Andrews *et al.*, 2007; Kumar and Pal, 2016).

1.4 Overlap extension PCR: An effective fusion method

In the late 20th century, fusion protein technology enabled the formation of chimeric proteins that combined functional domains from different sources. By joining two or more genes, the modified protein can be constructed with the desired traits, such as improving protein stability, valuability, or adding detection tags. Overlap extension PCR (OE-PCR) is a widely used fusion gene method that does not rely on restriction enzymes and ligation. It condenses the fusion process into three PCR reactions, allowing seamless junctions compared with the traditional restriction enzyme technique. First, each gene fragment was amplified separately by PCR using primers that added complementary overlapping sequences to the ends of the fragments. The PCR products were purified and added to the same reaction mixture as the calculated ratio. This fusion step forms the fusion DNA molecule through DNA fragments fused with other fragments in the correct orientation by annealing the overlapping regions. After fusion, the end-to-end primers were added to the PCR mixture to amplify

the full-length fusion product. Finally, a single continuous DNA sequence is formed that can encode the fusion protein.

OE-PCR involves the gene of interest at any desired junction, adding linker sequences, or inserting specific mutations or tags using well-designed primers. The high flexibility, cost efficiency, and simplicity of the fusion gene construction make it suitable for this project (Bryksin and Matsumura, 2010; Hashemabadi *et al.*, 2025).

1.5 Dual-function plasmid: The fusion of the selectable marker and reporter gene

By fusing the selectable marker and reporter gene, we constructed a dual-function plasmid that combines antibiotic resistance with fluorescent reporting. Dual-function plasmids are useful for genetic engineering and functional studies in a variety of organisms, such as bacteria and plants (Strathdee, McLeod and Underhill, 2000). The main purpose of fusing *NptII* and *mtsfGFP* genes is for simultaneous selection and real-time monitoring of the gene expression in the transformation process. Under the selective medium, only the cells that take up and express the fusion gene will survive antibiotic selection and emit fluorescence. The *NptII* gene allows resistance to aminoglycoside antibiotics by phosphorylating them, whereas *mtsfGFP* can directly visualize living transformed cells by emitting strong green fluorescence under UV or blue light (Das *et al.*, 2020; Andrews *et al.*, 2007).

By linking two genes, the occurrence of false-positive results is reduced and the reliability of transformation studies is increased. The researchers allow rapid identification of the true transformation, increasing the screening efficiency and saving time and resources. In addition, the dual-function plasmid achieved simultaneous qualitative and quantitative processes through survival in the selectable medium and the gene expression levels were assessed by measuring the intensity of *sfGFP* fluorescence. Based on this criterion, a comparison of the expression efficiency, transformation rates, or promoter strength across samples can be performed (Strathdee, McLeod and Underhill, 2000).

1.6 Objectives of this study

The main objective of this project was to construct a *NptII*-*mtsfGFP* fusion gene using overlap extension PCR.

The specific objectives of this project are as follows:

1. To fuse the target gene *mtNptII* in the pENTR- P_{COX1} :: *NptII*-T7TER plasmid and *mtsfGFP* in the pENTR- P_{COX2} -*mtsfGFP* plasmid.
2. To fuse the target gene *NptII* in the pENTR- P_{TEF1} -*NptII* plasmid and *mtsfGFP* in the pENTR- P_{COX2} -*mtsfGFP* plasmid.

CHAPTER 2

LITERATURE REVIEW

2.1 *Agrobacterium*-mediated transformation (AMT)

Agrobacterium-mediated transformation (AMT) is a fundamental technique in plant genetic engineering that utilizes the natural ability of the Gram-negative soil-borne phytopathogen *Agrobacterium tumefaciens* (*A. tumefaciens*), allowing the stable or transient insertion of a gene of interest (GOI) into various species. The transferred DNA (T-DNA) is a tumor-inducing (Ti) plasmid that is integrated into the host genome. It is the predominant tool for generating transgenic plants and contributes to the development of functional genomic studies in genetic engineering (Hwang, Yu, and Lai, 2017; De Saeger *et al.*, 2021). A significant breakthrough in genetic engineering occurred with the first successful AMT for plant transformation. However, a major challenge was the transfer of native T-DNA, which contains oncogenes, triggered crown gall disease in transformed plants through the formation of tumors. This problem was solved by subsequent research, in which disarmed vectors were engineered by removing these oncogenic genes while retaining the ability to transfer T-DNA. This crucial modification prevented tumorigenesis and

established AMT as an essential and practical tool for plant genetic engineering (Bourras, Rouxel and Meyer, 2015).

Compared with other plant transformation methods, it overcomes this obstacle and is able to pass through the impenetrable multi-layered plant cell, solving the most challenging barrier in plant transformation (Hwang, Yu, and Lai, 2017). Other methods, such as biolistic methods, electroporation, and microinjection, rely on mechanical forces to deliver DNA into plant cells. This method often causes irreparable cell damage and reduces transformation efficiency compared with AMT (Kumar and Ling, 2021).

AMT allows the delivery of large DNA fragments with low transgene copy numbers and minimal rearrangements, resulting in greater genetic stability. It is an artificially prepared Ti plasmid in the transfer DNA, or T-DNA region. Then, the helper plasmid carrying the virulence (*vir*) genes can transfer T-DNA into plant cells (De Saeger *et al.*, 2021).

2.1.1 Advances in AMT Methodology

In the beginning stage, native sequences from the T-DNA region, such as oncogenes and opine biosynthetic genes, were removed. The removal process eliminates its pathogenicity, but the ability of transgene delivery remains, forming the “disarmed” *A. tumefaciens* (Barton *et al.*, 1983).

In the past, researchers integrated a GOI into the disarmed Ti plasmid of *A. tumefaciens* through a modified *E. coli* plasmid, which serves as a shuttle vector via homologous recombination (HR) in the cointegration vector system. However, this system was shifted to a binary vector system because of its labor and complexity. This requires two cointegrating plasmids in *A. tumefaciens* (Barton *et al.*, 1983).

Over the years, researchers have discovered that the process of transferring T-DNA from *A. tumefaciens* will not be affected after separating the T-DNA region from the Ti plasmid, as long as the T-DNA and the Ti plasmid exist in the same *Agrobacterium* cell. Binary vector systems arose with the development of these studies. Based on the ability of GOI to be cloned into a smaller binary vector with a wide host range, this simplified molecular cloning system has become the standard method for AMT. Various *A. tumefaciens* strains and plasmid vectors have been developed to meet different research requirements (Tzfira and Citovsky, 2008).

2.1.2 Binary vector system

In AMT, the binary vector system acts as a modular plasmid system and is widely used because of its efficiency in delivering transgenes into the target host genomes. It includes two plasmids: a disarmed Ti plasmid containing the virulence (*vir*) genes that are essential for T-DNA transfer, and a separate small

binary vector containing the T-DNA region with the GOI flanked by left and right border sequences (Becker *et al.*, 1992).

The engineered binary vector can easily transfer foreign DNA into a variety of hosts, including plant or fungal cells, and is stably maintained by *Agrobacterium*. Selectable markers and multiple cloning sites exist for GOI insertions. The utility of this system was increased by constructing a Gateway-compatible binary vector with integrated Gateway cloning cassettes, such as *att* recombination sites and *ccdB* negative-selectable markers (Munaweera *et al.*, 2022).

Traditionally, the insertion of a GOI into a binary vector relies on conventional cloning methods, such as restriction enzymes and ligation, which are time-consuming and laborious. Gateway cloning is a site-specific recombination technology that enables seamless transfer of DNA fragments by recombination at *att* sites between vectors without requiring restriction sites, allowing bypassing of restriction-based cloning methods. The plasmid was introduced into *A. tumefaciens* after the recombinant binary vector was constructed in *E. coli*. Subsequently, *A. tumefaciens* mediates the transfer of the assembled T-DNA region into the host genome and undergoes stable integration and expression (Hwang, Yu and Lai, 2017)

In summary, binary vectors serve as the core T-DNA delivery and expression platform, and at the same time, Gateway cloning serves as an efficient cloning method that simplifies complex gene construction within the system. This

method reduces the cost, time, effort, and errors in cloning for ATM. Therefore, the binary vector system combined with Gateway cloning enhances the speed and flexibility of assembling and delivering transgenes into various hosts through *Agrobacterium* transformation (Karimi, Inzé and Depicker, 2002). This combination provides a powerful platform for research on genetic functions, expression, and subcellular localization to enhance genetic and molecular research in biological systems.

2.1.3 Engineered *Agrobacterium*-mediated transformation

In the AMT study, the destination vector carrying the GOI was expressed in the nucleus of the host cell. Based on my previous studies, an engineered AMT system was constructed that was able to transfer the GOI into the host's cell mitochondria. For transformation, a suitable entry vector capable of carrying the GOI and transforming it into mitochondria was built. Based on previous studies, the promoter of the plasmid was modified to initiate and express GOI, similar to the selectable marker. *^mNptII* is the modified version of *NptII*, which is only able to express inside the mitochondria, not inside the nucleus. This action efficiency eliminates the possibility that the GOI is accidentally expressed inside the nucleus, proving that the desired products are generated from the host's cell mitochondria. The fusion of *^mNptII* with the *sfGFP* gene allows the false positive result to be removed through observation of gene expression via growth on the selectable marker and visualization of the desired protein synthesis by fluorescent microscopy (Yap, 2025).

2.2 Gateway cloning

In recent years, the study of plant biological systems has relied on transgenic research by analyzing recombinant genes to a large extent using DNA cloning technologies. Unlike classical restriction-enzyme-based cloning methods, recombination cloning is an efficient and common cloning technology based on site-specific recombination. Without the requirement of a restriction site to insert the DNA sequence of interest, it allows rapid and efficient parallel transfer of the DNA of interest into diverse expression systems. One of the most popular recombination cloning technologies, Gateway cloning, allows the assembly of DNA fragments regardless of their sequence (Curtis and Grossniklaus, 2003).

Gateway cloning systems allow the joining of DNA fragments into a desired orientation and order and maintain their reading frame. This protocol relies on two main steps: a BP clonase reaction to insert the gene of interest (GOI) into an entry vector with an *attL* site. Lastly, the recombination of *attR* sites in the destination vector and *attL* sites in pENTR transfers the GOI into the expression vector via the LR reaction. For gene functional assay studies, a suitable destination vector can be recombined with a compatible entry clone

with an inserted GOI. The resulting expression clones were used for gene function testing, such as transformation into plants (Karimi, Depicker and Hilson, 2007).

2.2.1 Principle of Gateway cloning

First, the GOI, for instance, a PCR product flanked by two *attB* sites, is transferred into a donor vector (pDONR) by the BP *Clonase* II enzyme. It includes the integration host factor and phage integrase, which catalyze the BP reaction. The pDONR that carries two *attP* sites will recombine with *attB* sites on the GOI, allowing the GOI gene to be inserted into the donor backbone and form an entry plasmid (pENTR). pENTR is flanked by *attL* sites and is a key substrate in LR reactions. LR reaction is catalyzed by LR *Clonase* II enzymes, including phage excision, integration host factor, and integrase. It can transfer a GOI into an expression vector (pEXPR), which is flanked by *attB* sites, by recombination of *attL* sites on the entry vector and the destination vector (pDEST) carrying two *attR* sites. The researchers used pDONR, pENTR, pDEST, and pEXPR to differentiate the input and output plasmids in the cloning process (Curtis and Grossniklaus, 2003; Depicker and Hilson, 2007).

To maintain the open reading frame of the GOI, the engineered Gateway system alters the original *attB*, *attP*, *attL*, and *attR* sites to ensure specificity in

site-specific recombination. For example, *attB*1 reacts only with *attP*1, not *attP*2, to ensure directional cloning in this method. The entry vector is the key substrate in Gateway cloning and is generated by inserting the GOI into the pDONR flanked by *attL* sites. However, *attL* sites are relatively long (96 bp) and can interfere with applications that require minimal sequence addition, such as protein fusion or regulatory element spacing. In contrast, shorter *attB* sites (21-25 bp), specifically designed to lack translation initiation or stop codons, are more suitable for seamless cloning and expression constructs with minimal extra sequences. These sites function in the LR recombination step to generate an expression vector with *attB* sites in order to maintain the open reading frame of the GOI (Depicker and Hilson, 2007).

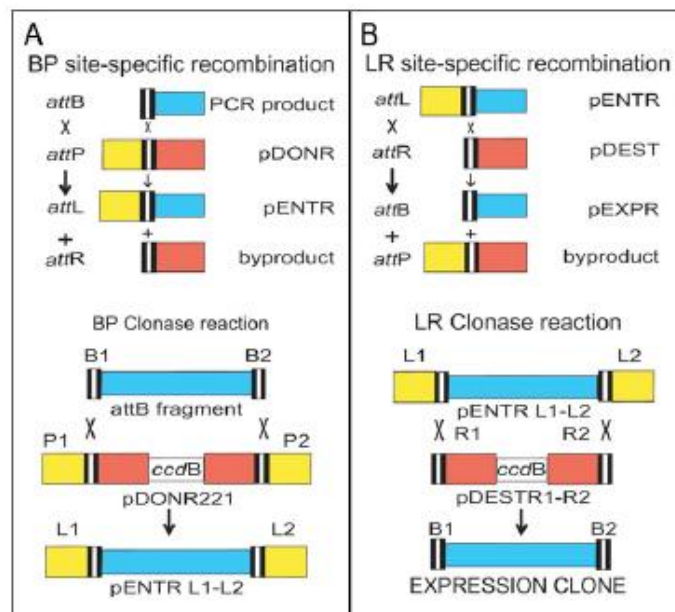


Figure 2.1: Schematic showing the flowchart of the Gateway cloning reaction. In part A, the BP clonase reaction, *attB* sites recombine with *attP* sites of the donor vector (pDONR). Then, a novel entry vector (pENTR) was generated and flanked by *attL* sites and the *attR* sides in the byproducts. In part B, the LR Clonase reaction, *attR* sites in the destination vector (pDEST) recombine with matching *attL* sites in the pENTR, generating

a novel expression vector (pEXTR) and *attP* as a byproduct (Depicker and Hilson, 2007).

Typically, ideal plasmids are constructed by *in vitro* recombination and transformed into *E. coli* strains. Through antibiotic selection and *ccdB* gene counterselection, the plasmid that successfully takes up the GOI can be segregated from the input vector and the reaction byproducts. Importantly, to avoid false-positive results in selection, different types of bacterial antibiotic resistance markers must be included in the plant binary T-DNA destination vector from the donor and entry vectors. Because of the kanamycin resistance that exists in most donor vectors used in the BP reaction, expression clones generated from the LR reaction should carry other selectable markers (Reece-Hoyes and Walhout, 2018).

In fact, *ccdB* is the toxic byproduct generated by Gateway cloning. It encodes a toxin that affects DNA replication by interfering with the bacterial DNA gyrase. DNA replication is inhibited and causes cell death when *ccdB* is expressed in *E. coli*. In the cloning process, the *ccdB* cassette will be replaced by a GOI through site-specific recombination. Only bacteria that successfully take up the replacement are able to survive and grow under selection conditions. Because *ccdB* kills the host cells without removing it, the background colonies containing non-recombinant or empty plasmids will be unable to survive (Lund *et.al*, 2014). Through negative selection, the screening burden was reduced and the recovery rate containing the desired recombinant construct increased. However, *ccdB* is toxic to ordinary *E. coli* strains. Hence, the engineered *E.*

E. coli strains that have mutated DNA gyrase are immune to the toxin, maintaining the stability of the vector containing *ccdB* before recombination. After recombination, plasmids are transformed into standard *E. coli* strains that are sensitive to *ccdB* toxicity (Reece-Hoyes and Walhout, 2018). Hence, this property is utilized in Gateway cloning of the cloning cassette in both donor and destination vectors within the *ccdB* gene.

2.2.2 Entry vector (pENTR)

Entry vectors (pENTR) are specially designed to serve as initial entrance for GOI in the Gateway cloning workflow. The GOI fragment flanked by *attB* sites recombines with the donor vector flanked by *attP* sites to form the pENTR vector with GOI and the toxic *ccdB* byproduct. The inserted DNA, flanked by the *attL1* and *attL2* recombination sites, can undergo further recombination into different destination vectors through the LR reaction. pENTR is a key component of gateway cloning because it is highly efficient and adaptable for high-throughput applications. Without requiring traditional restriction enzymes and ligation, GOI can easily shuttle between vectors for different downstream applications (Depicker and Hilson, 2007).

2.3 Neomycin phosphotransferase II (*NptII*): A Reliable Selectable Marker

Neomycin phosphotransferase II (NptII), which is isolated from the Tn5 transposon of *E. coli*, encodes an aminoglycoside phosphotransferase that resists aminoglycoside antibiotics such as kanamycin, G418, and neomycin. By phosphorylating aminoglycoside antibiotics, these antibiotics become inactive and lose the function that causes cell death (Das *et al.*, 2020). Thus, during the transformation process, the *NptII* selectable marker is transferred along with the GOI into the target host cell, thereby conferring antibiotic resistance to the transformants under selection (Numata *et al.*, 2016; Das *et al.*, 2020).

The presence of *NptII* in the aminoglycoside antibiotic G418 selectable medium affected the elongation step of translation to inhibit protein synthesis. In the transformed cells, the expression of the *NptII* gene inhibited the cytotoxic effect of G418; only the transformed cells survived. When *NptII* combines with G418, it specifically binds to the 30S ribosomal subunit in prokaryotes and organelles in eukaryotic cells (Miki and McHugh, 2004).

As a selectable marker, *NptII* is highly effective in screening transformed cells from non-transformed cells, thereby increasing the transformation selection speed. Even at low antibiotic concentrations, the *NptII*/G418 system undergoes effective selection, making this antibiotic resistance system highly reproducible and dependable. As the dominant selection system, *NptII* /G418 provides another option when auxotrophic selection is not available for wild-type and non-model organisms. It is widely used as a selectable marker gene in various organisms involved in prokaryotic and eukaryotic systems, from bacteria and

yeasts to plants and mammalian cells, with functions independent of the host metabolic background (Miki and McHugh, 2004; Mosey *et al.*, 2021).

2.3.1 Mitochondrial *NptII* (*^{mt}NptII*) : A modified version from *NptII*

Two distinct genomes exist in eukaryotic cells: the nuclear genome (nDNA) and mitochondrial genome (mtDNA). The nuclear genome contains thousands of genes, encodes most cellular proteins, and stores the genetic information of the organism. In contrast, mitochondrial DNA is a smaller circular DNA found within the mitochondria. It encodes essential proteins, tRNAs, and rRNAs. Most mitochondrially required proteins are imported after being encoded by the nucleus (Wiese and Bannister, 2020). Due to the difference in nuclear and mitochondrial genomes, *NptII* that expresses inside the nucleus after it integrates into the host's genome will not integrate into mitochondria and express. To overcome this problem, a modified *^{mt}NptII* gene was successfully constructed from *NptII*. Based on previous studies, *^{mt}NptII* was reliably integrated into the host mitochondrial genome and successfully expressed (Yap, 2025).

2.4 Green fluorescent protein (*GFP*)

Ormo *et al.* (1996) discovered a green fluorescent protein (*GFP*) in jellyfish (*Aequorea victoria*). He found that jellyfish emit green fluorescence but not

blue fluorescence. Theoretically, aequorin emits blue light when interacting with calcium ions. Based on this observation, he realized that another protein was involved. Through protein isolation, he obtained a second protein that emitted green fluorescence under UV light, which was named Green Fluorescent Protein (*GFP*). They also found that *GFP* can emit green fluorescence in the absence of a substrate or in the jellyfish cellular environment. Due to its non-invasive nature, *GFP* can be used as a reporter gene to visualize molecular activities within living cells.

2.4.1 GFP's three-dimensional structure

The GFP structure was characterized by Ormo et al. (1996) using X-ray crystallography; it is composed of 238 amino acids and has an approximate molecular weight of 27 kDNA. GFP has a distinctive beta-barrel fold in its tertiary structure, consisting of 11 beta strands and only one alpha strand. The β -strands are mostly arranged in an antiparallel orientation; each strand contains 9 to 13 amino acid residues and is stabilized by an extensive network of hydrogen bonds. The β -strands surround a central alpha helix, forming a cylindrical barrel conformation in the presence of hydrogen bonds. The barrel enclosed a highly protected internal environment for the GFP chromophore.

The alpha helix in the center of the barrel consists of only three amino acids: Ser65, Tyr66, and Gly67. These three residues produce a p-

hydroxybenzylideneimidazolidone chromophore through a series of post-translational autocatalytic modifications, including cyclization, dehydration, and oxidation. GFP's fluorescence is determined by folding the barrel structure. Almost all the sequences in the primary structure take part in the formation of the beta and alpha strands; therefore, it is difficult to remove them (Andrews *et al.*, 2007).

2.4.2 Mechanism of the chromophore

In GFP, green fluorescence occurs only when the protein folds into a tertiary beta-barrel structure. The primary amino acid sequences alone without folding do not emit any fluorescence. During folding, the alpha-strand amino acid residues Ser65, Tyr66, and Gly67 are incorporated into the barrel structure. Initially, the Ser65's carbonyl group undergoes nucleophilic attack by the amide nitrogen of Gly67. This process proceeds via cyclization to form a five-membered imidazolidone ring structure. Then, the water molecules were removed by dehydration. Lastly, the alpha-beta bond of Tyr66 is an oxidase that couples the aromatic group of Tyr66 with the imidazolidone ring to create a conjugated system. After post-translational chemical reactions, a mature chromophore for fluorescence was formed. Moreover, the unique environment of the beta-barrel structure protects the chromophore from solvent exposure and facilitates the correct conformational changes necessary through oxidation to confirm the maturation of the chromophore (Ormo *et al.*, 1996).

The mature chromophore can absorb two excitation peaks and emit visible light radiation. The major peak was at approximately 395 nm (UV light), and a minor peak was observed near 475 nm (blue light). Both excitation peaks, which are absorbed by the chromophore, cause an emission peak at approximately 508 nm, which corresponds to green fluorescence. This dual excitation feature allows *GFP* to be visualized under both blue and UV light, making it a convenient reporter gene (Barondeau *et al.*, 2003).

2.5 Mitochondrial superfolder green fluorescent protein (*sfGFP*)

The folding of GFP is an essential step for chromophore maturation and fluorescent emission. If the folding process is lacking, cyclization and oxidation reactions will not proceed and the chromophore will not be formed. The folding efficiency affects the fluorescence intensity of GFP. To address the limitations of wild-type GFP, superfolder GFP (*sfGFP*) was engineered to enhance folding robustness and fluorescence intensity. The mutated *sfGFP* was generated through Cycle3 mutations F99S, M153T, and V163A; the enhanced *GFP* mutations F64L and S65T; and six additional substitutions: S30R, Y39N, N105T, Y145F, I171V, and A206V. These mutations improve the performance of GFP by increasing its folding kinetics, solubility, and stability. The rate of protein misfolding and aggregation was reduced by Cycle3 mutations (Hsu,

Blaser and Jackson, 2009). However, the refolding efficiency of denatured protein reached a maximum of approximately 80%. However, based on the enhanced mutation and six additional mutations with Cycle3 mutations, sfGFP surpassed this limitation by achieving nearly 100% refolding efficiency, showing exceptional kinetic refolding and chemical resilience in various experiments. The excitation peak of sfGFP is at 450 nm, giving an emission peak at 508 nm, allowing bright green fluorescence to emit under blue light illumination. Importantly, sfGFP emits two-fold greater fluorescence intensity than wild-type GFP, enhancing the sensitivity for visualization and imaging applications (Pédélecq *et al.*, 2006).

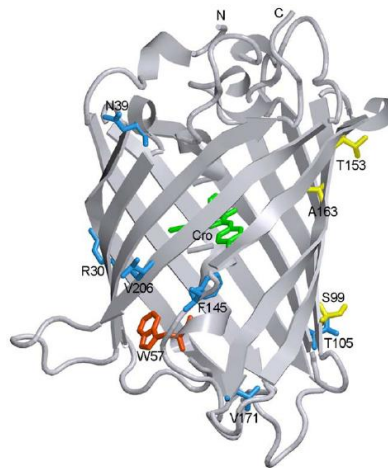


Figure 2.2: sfGFP's spatial structure. The green stick union is the location of the chromophore, and the red stick union shows the single tryptophan residue Trp57. Six mutation sites (S30R, Y39N, N105T, Y145F, I171V, and A206V) in cycle-3 are shown as blue stick unions. The mutations F99S, M153T, and V163A are shown in yellow stick unions (Pédélecq *et al.*, 2006).

CHAPTER 3

MATERIALS AND METHODS

3.1 Experimental workflow of the project

This section describes a method for constructing two sets of fusion genes. Both sets included the same core gene (*mtsfGFP*) and different partner genes (*NptII* or *mtNptII*). This study used overlap-extension PCR to join the target gene form into a single, continuous reading frame. The experimental workflow is shown as part A and part B for constructing the *NptII*-*mtsfGFP* and *mtNptII*-*mtsfGFP* fusion genes, respectively.

Part A: Construct *NptII*-*mtsfGFP* fusion gene

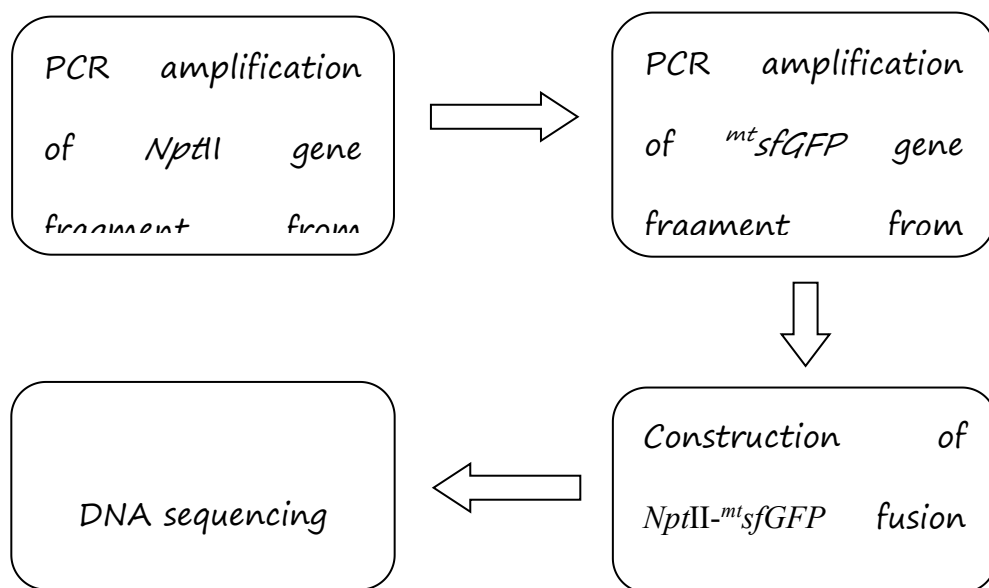


Figure 3.1: Experimental workflow of construct *NptII*-*mtsfGFP* fusion gene

Part B: Construct *mtNptII*-*mtsfGFP* fusion gene

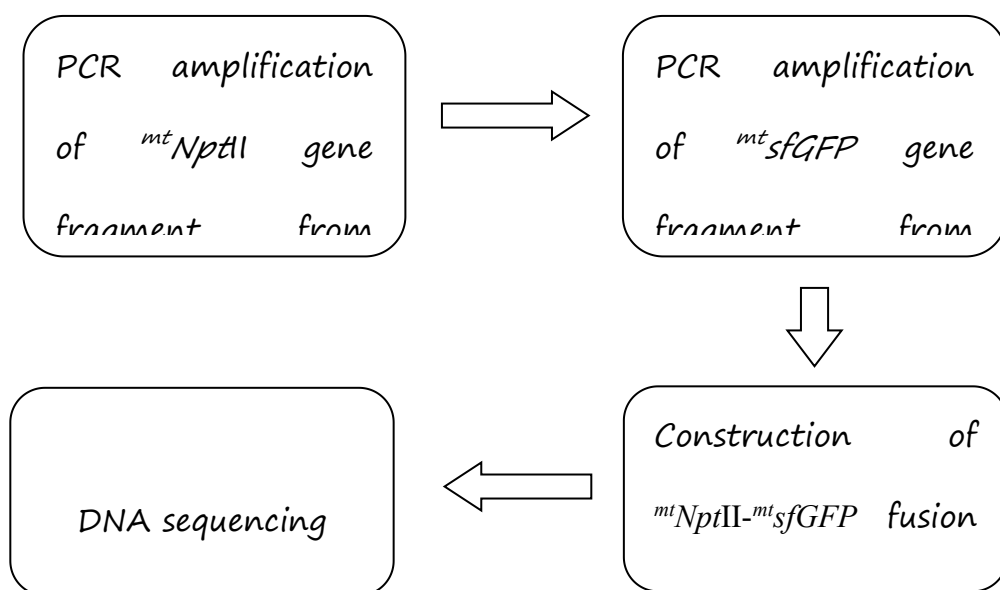


Figure 3.2: Experimental workflow of construct *mtNptII*-*mtsfGFP* fusion gene

3.2 Preparation of buffer, reagents and apparatus

In this final year project, all the chemical reagents and equipment were provided by Department of Biological Science, Faculty of Science of Universiti Tunku Abdul Rahman (UTAR) and my supervisor Prof. Dr. Wong Hann Ling, as listed in Appendices A.

3.2.1 Preparation of 5X Tris/Borate/EDTA (TBE) buffer

0.5 M of EDTA was prepared in a 5X TBE buffer. An amount of 18.61 g EDTA disodium salt (FW: 372.2 g/mol) was dissolved in 80 mL of dH₂O. The solution was colorless when adjusted to pH8 using 5M NaOH. For the preparation of the 1 L 5X TBE buffer, 5.4 g of tris base (MW: 121.14 g/mol) and 27.5 g of boric acid (FW: 61.83 g/mol.) was dissolved in 800 mL dH₂O. The solution was topped up to 1 L after adding 20 mL of 0.5 M EDTA solution.

3.2.2 Preparation of 3 M sodium acetate (NaOAc) solution

Fifty mL of 3M NaOAc solution was used as the essential solution for ethanol precipitation. 12.30 g of sodium acetate (MW: 82.03 g/mol) was dissolved in a beaker containing 30 mL of dH₂O. Then, the pH of the solution was adjusted to pH 5.2 with glacial acetic acid. Finally, the volume of the solution was increased to fifty mL using dH₂O.

3.3 Agarose gel electrophoresis

The PCR products were verified by agarose gel electrophoresis. The 5X TBE was diluted to $0.5 \times$ TBE buffer with dH_2O , which served as the running buffer, and the agarose gel was cast. The percentage of agarose gel electrophoresis was determined based on the desired size of the DNA fragment. A larger DNA fragment size required a lower percentage of agarose gel. To verify the PCR product from single primer amplification and target gene amplification below 1500 bp, a 1.2% agarose gel was cast. Agarose gel powder (0.48 g) was added to 40 mL of $0.5 \times$ TBE and completely dissolved in the solution after being heated in a microwave. Then, gel stain (Dye AllTM) was added to the solution when it slightly cooled. After that, the mixed solution was poured into the gel casting set and left to settle and solidify. This took approximately 40 min. Next, the gel was run in $0.5 \times$ TBE buffer at 100 V for 35 min and viewed under a UV transilluminator.

To verify the larger amplicon (> 1500 bp) from overlap extension PCR, a 0.8% agarose gel was cast. The agarose gel electrophoresis process was the same as that used for 1.2% agarose gel electrophoresis, except that the amount of agarose powder was decreased to 0.32 g.

3.4 Purification of PCR fragment using EZ-10 Spin Column DNA Gel

Extraction Kit

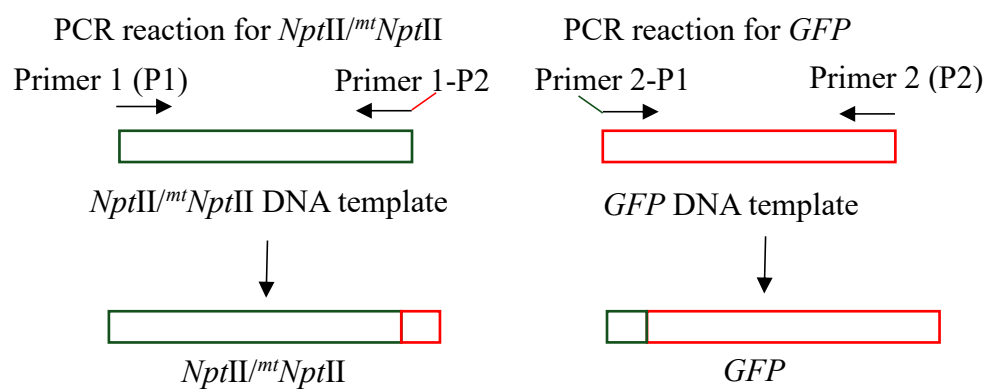
The PCR product was purified using the EZ-10 spin column DNA gel extraction kit. After the target band location was confirmed by comparison with the DNA ladder under a UV transilluminator, gel excision was performed. The

target band was cut from the agarose gel by using a sterile scalpel. The weight of the gel slice was then placed into a 1.5 mL microcentrifuge tube and measured using an electronic weighting scale. Next, the binding buffer was added to the same 1.5 mL microcentrifuge tube. The volume of binding buffer added followed the rules, in which 200 μ L of binding buffer was added to each 100 mg of agarose gel. The sample was then incubated in a preheated heat block at 50 °C until the gel slice completely melted. The sample was vortexed every 3 min to evenly mix the binding buffer and gel slice, and the gel slice melting process was accelerated. The EZ-10 column was placed in a 2.0 mL collection tube first when cooling down the mixture at room temperature. A volume of 700 μ L of the mixture was transferred to the column and centrifuged at $11,000 \times g$ for 30 s. The flow-through was discarded, and 700 μ L of washing buffer was added to the column. Then, the flow-through was discarded after centrifugation at $11,000 \times g$ for 30 s. The washing steps were repeated to minimize the chaotropic salt and improve the A_{260}/A_{230} values. The column containing the collection tube was centrifuged at $11,000 \times g$ for 1 min to completely remove the washing buffer. The column was transferred to a new 1.5 mL microcentrifuge tube. Subsequently, 30 μ L of preheated elution buffer was pipetted directly onto the center of the membrane and fully covered the membrane surface to improve the elution efficiency of the bound DNA. The column was incubated at room temperature for 1 min before centrifugation at $11,000 \times g$ for 1 min. The bound DNA was eluted and the concentration was measured using a NanoDrop. Finally, the extracted DNA was stored at -20°C freezer until further use.

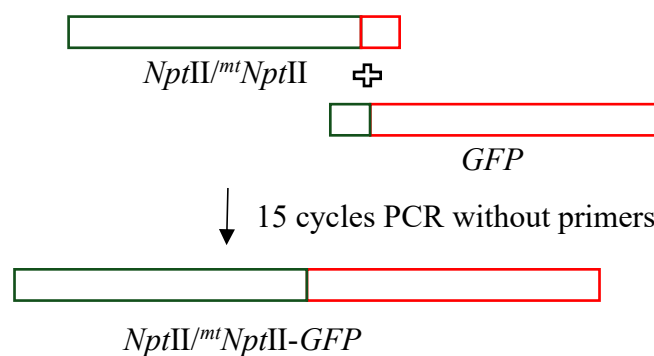
3.5 Construction of *NptII*^{mt}*NptII*-*mt*sfGFP fusion gene

3.5.1 Graphical overview of fusion gene construction

Step 1: Amplification of primary fragments



Step 2: Overlap PCR reaction



Step 3: Final fusion gene PCR amplification

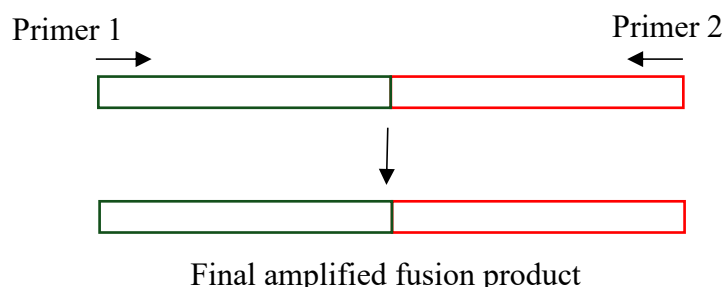


Figure 3.1: Graphical overview of constructing the *NptII^{mt}NptII^{mt}sfGFP* fusion gene by overlap extension PCR. In step 1 (top panel), target gene fragments containing overlapping regions were amplified by PCR. Step 2 (middle panel) uses the *NptII^{mt}NptII* and *mtsfGFP* gene fragments to generate the full-length *NptII^{mt}NptII^{mt}sfGFP* fusion gene by overlap extension PCR. Step 3: Final PCR amplification of the full-length *NptII^{mt}NptII^{mt}sfGFP* fusion gene as the final product with the outermost primer.

3.5.2 Megaprimer Design

Megaprimers were designed to generate the *NptII^{mt}NptII^{mt}sfGFP* fusion gene. The target fusion gene that contains the overlap region was integrated into a single, continuous reading frame through overlap PCR. For successful fusion, the stop codon at the end of *NptII^{mt}NptII* was removed and only located at the end of *mtsfGFP*. Both megaprimers shown in the overlap region contained fused sequences that were complementary to each other, ensuring precise amplification and incorporation of the overlapping segment necessary for efficient gene fusion. To construct the *NptII^{mt}NptII^{mt}sfGFP* fusion gene, the reverse megaprimer (R-OPCR-*NptII^{mt}sfGFP*/R-OPCR-*mtNptII^{mt}sfGFP*) for amplifying the *NptII^{mt}NptII* gene contains the *mtsfGFP* gene sequence. The forward primer (F-OPCR-*NptII^{mt}sfGFP* /F-OPCR-*mtNptII^{mt}sfGFP*) contains

the end of *NptII*^{mt}*NptII* gene sequence before starting to amplify the *mtsfGFP* gene sequence. The primer sequences are listed in Tables 3.1, 3.2, and 3.3.

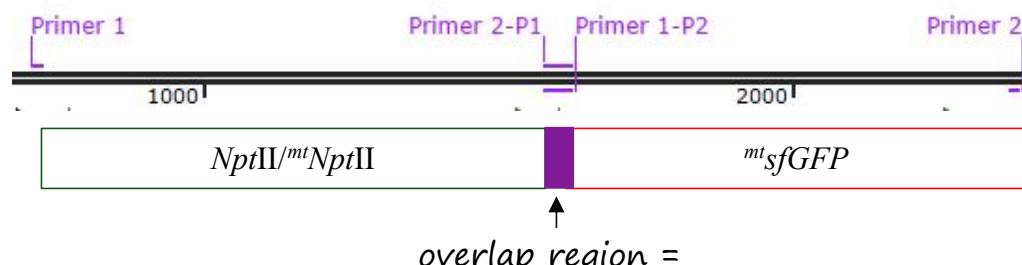


Figure 3.2: Schematic diagram showing megaprimer design to construct the *NptII*^{mt}*NptII*-*mtsfGFP* fusion gene. The designed megaprimer introduces an overlap region that contain a 55 bp sequence, labeled as a purple region, for seamless fusion by overlap extension PCR. Both primers shown in the figure were positioned to flank their respective target sequences. The reverse primer was designated as primer 1-P2 and the forward primer was labeled as primer 2-P1.

Table 3.1: Nucleotide sequence of primers used to amplify the *NptII* gene fragment from the pENTR-P_{TEF1}-*NptII* plasmid.

Primer	Sequences (5'...3')
F- <i>attL</i> - <i>NotI</i>	CAACTTTGTACAAAAAAGCAGGCT
R-OPCR- <i>NptII</i> - <i>mtsfGFP</i>	<u>GAATAATTCTTCACCTTTAGACATGGTCTCG</u> <u>GATCCGAAAAACTCATCGAGCATC</u>

* Underlined sequences indicate overhanging regions.

Table 3.2: Nucleotide sequences of primers used to amplify *mtNptII* gene fragments from the pENTR-P_{Cox1}-*mtNptII* plasmid.

Primer	Sequences (5'...3')
F- <i>attL</i> - <i>NotI</i>	CAACTTTGTACAAAAAAGCAGGCT
R-OPCR- <i>mtNptII</i> - <i>mtsfGFP</i>	<u>GAATAATTCTTCACCTTTAGACATGGTCTC</u>

GGATCCGAAGAACTCGTCCAACATC

* Underlined sequences indicate overhanging regions.

Table 3.3: Nucleotide sequences of primers used to amplify the *mtsfGFP* gene fragment from pENTR-*P_{Cox2}*-*mtsfGFP* plasmid.

Primer	Sequences (5'...3')
F-OPCR- <i>NptII</i> - <i>mtsfGFP</i>	<u>GATGCTCGATGAGTTTTTCGGATCCGAGA</u> CCATGTCTAAAGGTGAAGAATTATTC
F-OPCR- <i>mtNptII</i> - <i>mtsfGFP</i>	<u>GATGTTGGACGAGTTCTTCGGATCCGAGA</u> <u>CCATGTCTAAAGGTGAAGAATTATTC</u>
R-T7-Ter-AscI	GGCGCGCCCCACCCTTCAAAAAAC

* Underlined sequences indicate overhanging regions.

3.5.3 Single-Primer Amplification Test with DNA Template

To eliminate false positive results, a single primer was tested by PCR with the related DNA template. Due to the *mtsfGFP* gene fragment fuses with different gene fragments, it was tested with different pairs of primers. The data from this section will contribute to further modifications of the PCR conditions. The PCR reagent components and thermocycling parameters are listed in Tables 3.3, 3.4, and 3.5, respectively.

Table 3.4: PCR master mix and reaction components with their corresponding volumes.

Component	Stock concentration	Final concentration	Volume (μL)
-----------	------------------------	------------------------	-------------

Vayzme 2X Taq	2X	1X	5
master mix			
Forward primer/	10 μ M	0.3 μ M	0.3
Reverse primer			
DNA template	50 ng/ μ L	1 ng/ μ L	0.2
Sterile distilled			
water	-	-	4.2
Total volume	-	-	10

Table 3.5: PCR thermocycling parameters for *mtNptII* and *mtsfGFP* single primer testing with the extracted pENTR-P_{Cox1}-*mtNptII* and pENTR-P_{Cox2}-*mtsfGFP* plasmids, respectively.

Reaction	Temperature (°C)	Time	Numbers of cycles
Initial denaturation	95	3 min	1
Denaturation	95	15 sec	25
*Annealing	56	15 sec	
	53	15 sec	
Extension	72	1 min	
Final extension	72	5 min	1
Hold	4	∞	-

* For *mtNptII* and *mtsfGFP*(*mtNptII*) single-primer testing, the annealing temperature was set at 56°C. For *mtsfGFP*(*NptII*) single-primer testing, the annealing temperature was set to 53°C.

Table 3.6: PCR thermocycling parameters for NptII single-primer amplification with the extracted pENTR-p_{TEF1}-NptII plasmid.

Reaction	Temperature (°C)	Time	Numbers of cycles
Initial denaturation	95	3 min	1
Denaturation	95	15 sec	20
Annealing	56	15 sec	
Extension	72	1:30 min	
Final extension	72	5 min	1
Hold	4	∞	-

3.5.4 PCR amplification of *NptII*, *^{m1}NptII* and *^{m1}sfGFP* gene fragment

The first PCR amplification generates amplicons that contain overlapping sequences for further overlap extension PCR, as described in Section 3.5.5. To increase the efficiency of PCR, the thermocycling parameters for fragment amplification were modified based on the results of the single-primer amplification test. The primer sets, PCR components, and thermocycling parameters are summarized in Tables 3.1, 3.2, 3.3, 3.6, 3.7, and 3.8, respectively.

Table 3.7: PCR master mix and reaction components with their corresponding volumes.

Component	Stock	Final	Volume (μL)
-----------	-------	-------	-------------

	concentration	concentration	
Vayzme 2X Taq master mix	2X	1X	25
Forward primer	10 μ M	0.3 μ M	1.5
Reverse primer	10 μ M	0.3 μ M	1.5
DNA template	50 ng/ μ L	1 ng/ μ L	1
Sterile distilled water	-	-	21
Total volume	-	-	50

Table 3.8: PCR thermocycling parameters for amplifying *NptII* with the extracted pENTR- P_{TEF1} -*NptII* plasmid.

Reaction	Temperature ($^{\circ}$ C)	Time	Numbers of cycles
Initial denaturation	95	3 min	1
Denaturation	95	15 sec	20
Annealing	56	15 sec	
Extension	72	1:30 min	
Final extension	72	5 min	1
Hold	4	∞	-

Table 3.9: PCR thermocycling parameters for amplifying *mtNptII/mtsfGFP* with the extracted pENTR-*P_{Cox1}-mtNptII*/pENTR-*P_{Cox2}-mtsfGFP* plasmid.

Reaction	Temperature (°C)	Time	Numbers of cycles
Initial denaturation	95	3 min	1
Denaturation	95	15 sec	25
	53	15 sec	
*Annealing	56		
	60		
Extension	72	1 min	
Final extension	72	5 min	1
Hold	4	∞	-

* For the amplified *mtsfGFP(NptII)* the annealing temperature was set to 53°C.

* For the amplified *mtNptII*, the annealing temperature was set to 56°C.

* For the amplified *mtsfGFP(mtNptII)*, the annealing temperature was set to 60°C.

3.5.5 Overlap extension PCR for *NptII/mtNptII-mtsfGFP* fusion gene construction

The purpose of the overlap extension PCR was to obtain the full-length *NptII/mtNptII-mtsfGFP* fusion gene. In this PCR reaction, no primer was used, and it relied on the purified PCR product generated in Section 3.5.4. First, the PCR products were verified by agarose gel electrophoresis (Section 3.3) and then purified as described in Section 3.4. The purified *NptII/mtNptII* and *mtsfGFP* genes were diluted and the molar ratio of the DNA template was calculated using the Vayzme calculator, followed by each fragment bp size. The larger the fragment size, the larger the amount of input DNA. The PCR

components and thermocycling parameters are presented in Tables 3.9, 3.10, and 3.11, respectively.

Table 3.10: PCR master mix and reaction components with their corresponding volumes for the *NptII*-*mtsfGFP* fusion gene.

Component	Stock concentration	Final concentration	Volume (μL)
Vayzme 2X Taq master mix	2X	1X	25
DNA template - <i>NptII</i>	1 ng/ μL	0.15 ng/ μL	7.5
DNA template - <i>mtsfGFP</i>	1 ng/ μL	0.1 ng/ μL	5

Sterile distilled water	-	-	9.5
Total volume	-	-	47

Table 3.11: PCR master mix and reaction components with their corresponding volumes for *mtNptII*-*mtsfGFP* fusion gene.

Component	Stock concentration	Final concentration	Volume (μL)
Vayzme 2X Taq master mix	2X	1X	25
DNA template - <i>mtNptII</i>	1 ng/ μL	0.15 ng/ μL	7.5
DNA template - <i>mtsfGFP</i>	1 ng/ μL	0.135 ng/ μL	6.75

Sterile distilled	-	-	7.75
water	-	-	
Total volume	-	-	47

Table 3.12: PCR thermocycling parameters for constructing the *NptII^{mt}NptII^{mt}sfGFP* fusion gene.

Reaction	Temperature (°C)	Time	Numbers of cycles
Initial denaturation	95	3 min	1
Denaturation	95	15 sec	15
Annealing	60	15 sec	
Extension	72	30 sec	
Final extension	72	5 min	1
Hold	4	∞	-

3.5.6 Final *NptII^{mt}NptII^{mt}sfGFP* fusion gene PCR amplification

Full-length *NptII^{mt}NptII^{mt}sfGFP* fusion gene was amplified for further DNA cloning. Due to both amplified fragments have an overlap region, they fuse together in section 3.5.5. Subsequently, the primers were added directly to the same PCR mixture for amplification. The *NptII^{mt}NptII^{mt}sfGFP* fusion gene was amplified using the same outer primer set. The primer set, number of added primers, and thermocycling parameters are listed in Tables 3.12, 3.13, 3.14, and 3.15, respectively.

Table 3.13: Nucleotide sequences of the outer primers used to amplify the *NptII^{mt}NptII^{mt}sfGFP* fusion gene fragment.

Primer	Sequences (5'...3')
F- <i>attL</i> - <i>NotI</i>	CAACTTTGTACAAAAAAGCAGGCT
R-T7-Ter- <i>AscI</i>	GGCGCGCCCACCCTTCAAAAAAC

Table 3.14: PCR mixtures and primers added with their corresponding volumes.

Component	Stock concentration	Final concentration	Volume (μL)
PCR mixture	-	-	47
Forward primer	10 μM	0.3 μM	1.5
Reverse primer	10 μM	0.3 μM	1.5
Total volume	-	-	50

Table 3.15: PCR thermocycling parameters for amplifying the *NptII^{mt}sfGFP* fusion gene.

Reaction	Temperature (°C)	Time	Numbers of cycles
Initial denaturation	95	3 min	1
Denaturation	95	15 sec	25
Annealing	59	15 sec	
Extension	72	2:30 min	
Final extension	72	5 min	1

Hold	4	∞	-
------	---	----------	---

Table 3.15: PCR thermocycling parameters for amplifying the *^{mt}NptII-^{mt}sfGFP* fusion gene.

Reaction	Temperature (°C)	Time	Numbers of cycles
Initial denaturation	95	3 min	1
Denaturation	95	15 sec	25
Annealing	60	15 sec	
Extension	72	2 min	
Final extension	72	5 min	1
Hold	4	∞	-

3.6 Purification of *NptII-^{mt}sfGFP* fusion gene fragment

For further DNA cloning, purification is required to remove impurities in the PCR products, such as salt, residual primers, and non-specific amplification products. DNA purity increases the efficiency of cloning. First, the PCR product was verified using 0.8% agarose gel electrophoresis, as described in Section 3.3. The target PCR product was purified following the steps described in Section 3.4. After purification, the purified DNA was stored at -20°C for further use.

3.7 Purification of *mtNptII-mtsfGFP* fusion gene fragment

3.7.1 Low-melting agarose gel electrophoresis

To easily extract the desired DNA fragment from the agarose gel, a low-melting agarose gel was used. The criteria for this type of agarose gel were utilized to make it easier to dissolve in dH₂O at moderate temperatures (~60°C). First, 0.2 g of low-melting agarose powder was weighed and dissolved in 0.5X TBE buffer. The subsequent process preparation of 1.0% low-melting agarose gel was identical to that of normal agarose gel preparation in section 3.4. The gel was run in 0.5 ×TBE buffer at 100 V for 35 min and viewed under a UV transilluminator.

3.7.2 Ethanol precipitation for gel purification

The amplified *mtNptII-mtsfGFP* fusion gene product was purified by ethanol precipitation. The target band on the gel was cut using a sterile scalpel after the target band location was confirmed using a UV transilluminator. Next, the gel slice was collected into a 1.5 mL microcentrifuge tube with 500 µL of dH₂O. The microcentrifuge tube was incubated in a preheated heat block at 50 °C. To completely dissolve the gel slice, the microcentrifuge tube was vortexed

every 2 minutes. The supernatant (500 μ L) was transferred into a new 1.5 mL microcentrifuge tube. 1 mL of phenol-chloroform-isoamyl alcohol (PCI) mixture was added inside, and the mixture was vortexed for 2 minutes. The microcentrifuge tube was then centrifuged at 12,500 rpm and 4°C for 10 min in a pre-cold low-temperature centrifuge. Five hundred microliters of supernatant were transferred into a new 1.5 mL microcentrifuge tube; the buffy coat was carefully avoided during collection to improve DNA purity and minimize contamination. Next, 50 μ L of 3 M NaOAc solution and 500 μ L of ice-cold 100% EtOH were added. To improve DNA sedimentation, the solution was gently mixed and placed in a -20°C freezer overnight. The next day, the solution was centrifuged at 12,500 rpm at 4°C for 30 min in a pre-cooled low-temperature centrifuge to obtain the DNA pellet. The supernatant was discarded and 1 mL of ice-cold 100% EtOH was pipetted into a microcentrifuge tube for pellet washing. Next, the supernatant was discarded and the remaining supernatant was pipetted. The whitish pellet became transparent after being fully air-dried. Finally, the pellet was fully dissolved in 30 μ L of dH₂O, and the concentration of extracted DNA was measured using a NanoDrop spectrophotometer. For long-term storage, the extracted DNA was stored at -20°C until further use.

3.8 DNA sequencing

The fusion gene product was purified and stored as extracted DNA in a -20°C freezer. For both fusion gene products, *NptII-m^tsfGFP* and *m^tNptII-m^tsfGFP*, the size was over 1500 bp. For 1st BASE company DNA sequencing, the required concentration of DNA, which was over 1500 bp, was 30 ng/ μ L. Both fusion genes reached the concentration requirement, but the purity of the *m^tNptII-*

mtsfGFP fusion gene did not meet this requirement. Twenty microliters of the extracted DNA and 10 µL of forward and reverse primers were used for sequencing.

CHAPTER 4

RESULT

4.1 Construction of *NptII*^{mt}*NptII*-^{mt}*sfGFP* fusion gene

4.1.1 Megaprimer Design

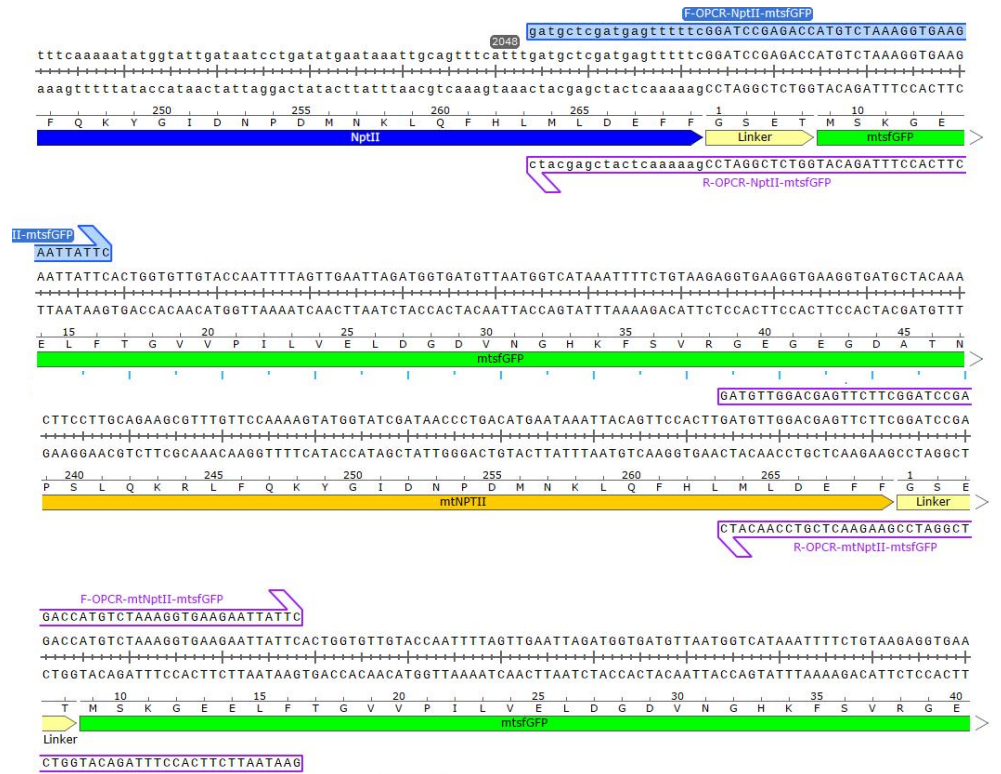


Figure 4.1: Schematic showing the sequence of the *NptII*^{mt}*NptII*-^{mt}*sfGFP* fusion gene. Megaprimers were designed to cross the *NptII*^{mt}*NptII* and *mtsGFP* gene fragments. The overlapping regions were complementary to each other. The stop codon in *NptII*^{mt}*NptII* was removed. The full length of both forward and reverse megaprimers was 55 bp, and Tm was 69°C.

A) Potential hairpin formation :

5' GATGCTCGATGAGTTTTTCGGATCCGAGACCATGTCTAAAGGTGAAGAATTATTC 3'

3' Complementarity:
None !

All potential self-annealing sites are marked in red (allowing 1 mis-match):

5' GATGCTCGATGAGTTTTTCGGATCCGAGACCATGTCTAAAGGTGAAGAATTATTC 3'
3' CTTATTAGAAGTGGAAATCTGTACCAGAGCCTAGGCTTTTGTAGTACGCTGTAG 5'

Potential hairpin formation :

5' GATGTTGGACGAGTTCTTCGGATCCGAGACCATGTCTAAAGGTGAAGAATTATTC 3'

3' Complementarity:
None !

All potential self-annealing sites are marked in red (allowing 1 mis-match):

5' GATGTTGGACGAGTTCTTCGGATCCGAGACCATGTCTAAAGGTGAAGAATTATTC 3'
3' CTTATTAGAAGTGGAAATCTGTACCAGAGCCTAGGCTTTTGTAGCAGGTTGTAG 5'

5' GATGTTGGACGAGTTCTTCGGATCCGAGACCATGTCTAAAGGTGAAGAATTATTC 3'
3' CTTATTAGAAGTGGAAATCTGTACCAGAGCCTAGGCTTTTGTAGCAGGTTGTAG 5'

5' GATGTTGGACGAGTTCTTCGGATCCGAGACCATGTCTAAAGGTGAAGAATTATTC 3'

3' CTTATTAGAAGTGGAAATCTGTACCAGAGCCTAGGCTTTTGTAGCAGGTTGTAG 5'

B)

5' GATGTTGGACGAGTTCTTCGGATCCGAGACCATGTCTAAAGGTGAAGAATTATTC 3'
3' CTTATTAGAAGTGGAAATCTGTACCAGAGCCTAGGCTTTTGTAGCAGGTTGTAG 5'

5' GATGTTGGACGAGTTCTTCGGATCCGAGACCATGTCTAAAGGTGAAGAATTATTC 3'
3' CTTATTAGAAGTGGAAATCTGTACCAGAGCCTAGGCTTTTGTAGCAGGTTGTAG 5'

C)

5' GATGTTGGACGAGTTCTTCGGATCCGAGACCATGTCTAAAGGTGAAGAATTATTC 3'
3' CTTATTAGAAGTGGAAATCTGTACCAGAGCCTAGGCTTTTGTAGCAGGTTGTAG 5'

D) Potential hairpin formation :

```

5' GAATAATTCTTCACCTTTAGACATGGTCTCGGATCCGAAGAACTCGTCCAACATC 3'
5' GAATAATTCTTCACCTTTAGACATGGTCTCGGATCCGAAGAACTCGTCCAACATC 3'
5' GAATAATTCTTCACCTTTAGACATGGTCTCGGATCCGAAGAACTCGTCCAACATC 3'

```

3' Complementarity:
None !

All potential self-annealing sites are marked in red (allowing 1 mis-match):

```

5' GAATAATTCTTCACCTTTAGACATGGTCTCGGATCCGAAGAACTCGTCCAACATC 3'
3' CTACAACCTGCTCAAGAAGCCTAGGCTCTGGTACAGATTCCACTTCTTAATAAG 5'

5' GAATAATTCTTCACCTTTAGACATGGTCTCGGATCCGAAGAACTCGTCCAACATC 3'
3' CTACAACCTGCTCAAGAAGCCTAGGCTCTGGTACAGATTCCACTTCTTAATAAG 5'

5' GAATAATTCTTCACCTTTAGACATGGTCTCGGATCCGAAGAACTCGTCCAACATC 3'
3' CTACAACCTGCTCAAGAAGCCTAGGCTCTGGTACAGATTCCACTTCTTAATAAG 5'

5' GAATAATTCTTCACCTTTAGACATGGTCTCGGATCCGAAGAACTCGTCCAACATC 3'
3' CTACAACCTGCTCAAGAAGCCTAGGCTCTGGTACAGATTCCACTTCTTAATAAG 5'

5' GAATAATTCTTCACCTTTAGACATGGTCTCGGATCCGAAGAACTCGTCCAACATC 3'
3' CTACAACCTGCTCAAGAAGCCTAGGCTCTGGTACAGATTCCACTTCTTAATAAG 5'

5' GAATAATTCTTCACCTTTAGACATGGTCTCGGATCCGAAGAACTCGTCCAACATC 3'
3' CTACAACCTGCTCAAGAAGCCTAGGCTCTGGTACAGATTCCACTTCTTAATAAG 5'

```

Figure 4.2: Analysis of megaprimer secondary structure using an Oligonucleotide Properties Calculator. In the megaprimer design for the *NptII-mt⁺sfGFP* fusion gene: A) Forward megaprimer: F-OPCR-*NptII-mt⁺sfGFP* shows the potential for one hairpin formation and five self-annealing sites; B) Reverse megaprimer: R-OPCR-*NptII-mt⁺sfGFP* shows the potential for two hairpin formation and five self-annealing sites. In the megaprimer design for the *mtNptII-mt⁺sfGFP* fusion gene: C) Forward primer: F-OPCR-*mtNptII-mt⁺sfGFP* shows the potential for one hairpin formation and six self-annealing sites; D) Reverse megaprimer: R-OPCR-*mtNptII-mt⁺sfGFP* shows the potential for three hairpin formations and six self-annealing sites.

4.2



Single primer amplification test with DNA template

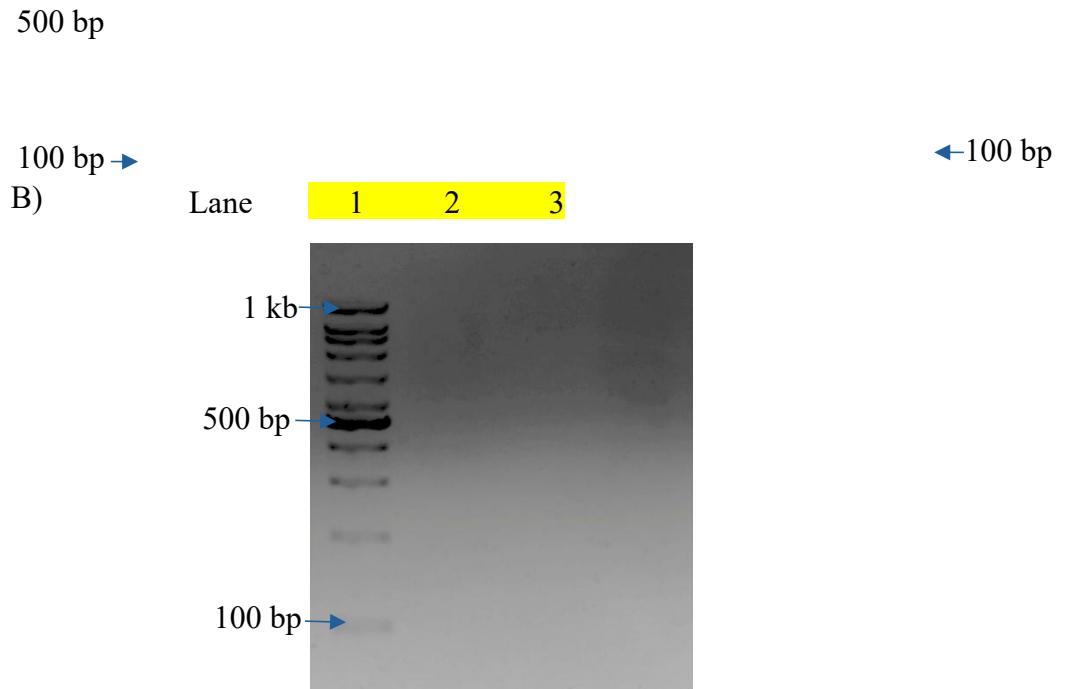


Figure 4.3: Inverted 1.2% agarose gel image from the single-primer amplification test with the corresponding DNA template. The gel images were digitally inverted to enhance band contrast for better visualization and assessment of product absence. In part A, three sets of single primer testing are illustrated: lanes 2 and 3 correspond to reactions using primers F-*attL-NotI* and R-OPCR- *mtNptII-mt sfGFP*; lanes 4 and 5 show F-OPCR-*mtNptII-mt sfGFP* and R-T7-Ter-*AscI*; and lanes 6 and 7 display F-OPCR- *NptII-mt sfGFP* and R-T7-Ter-*AscI*. Lanes 1 and 8 contain the 100 bp DNA ladder as a molecular weight marker. In part B, a 1 kb DNA ladder was used in lane 1, suitable for the 1402 bp *NptII* gene fragment. The PCR conditions were optimized to ensure no detectable bands in any of the single primer reactions, confirming the specificity of the amplification conditions shown in the figure.

4.3. PCR amplification of gene fragment

4.3.1 *NptII*, *mtNptII*, and *mtsfgGFP* gene fragments

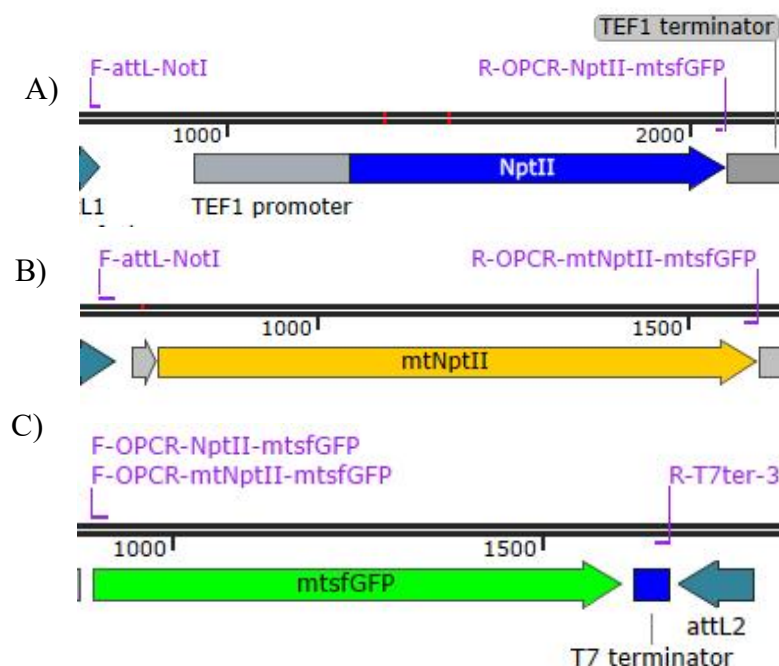


Figure 4.4: Schematic showing the sequence of the *NptII*, *mtNptII*, and *mtsfgGFP* gene fragments with their primers. In part A, *NptII* sequences was amplified by F-attL-NotI and R-OPCR- *NptII*-*mtsfgGFP* primer set, R-OPCR-*NptII*-*mtsfgGFP* contain the overhanging region complementary with *mtsfgGFP*. In part B, *mtNptII* sequences was amplified by F-attL-NotI and R-OPCR-*mtNptII*-*mtsfgGFP* primer set, R-OPCR-*mtNptII*-*mtsfgGFP* contain the overhanging region complementary with *mtsfgGFP*. In part C, *mtsfgGFP* was amplified with difference forward primer, which were F-OPCR-*NptII*-*mtsfgGFP* and F-OPCR-*mtNptII*-*mtsfgGFP* to create different overhanging region for further fusion step, reverse primer was R-T7-Ter-AscI.

4.3.2 Result of agarose gel electrophoresis

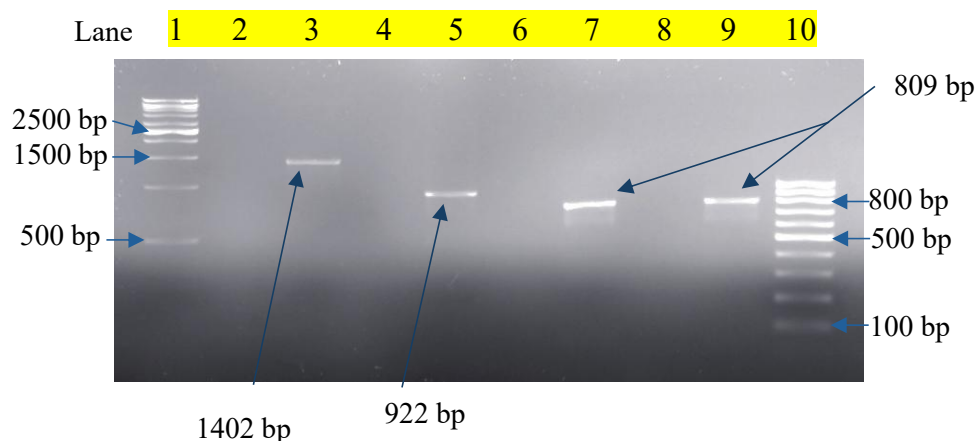


Figure 4.5: PCR amplification for *NptII*, *mtNptII*, and *mtsfgFP* gene fragments was electrophoresed on a 1.2% (w/v) agarose gel. Lane 1 contains the 1 kb DNA ladder as a molecular weight marker, followed by lane 2 containing the negative control for the *NptII* gene fragment. Lane 3 shows a successfully amplified *NptII* fragment at 1402 bp. Lane 4 contains the negative control for the *mtNptII* gene fragment, whereas lane 5 presents the amplified *mtNptII* gene fragment at 922 bp. Lane 6 contains the negative control for the *mtsfgFP* (*NptII*) gene fragment and lane 7 displays its amplified product at 809 bp. Lane 8 contains the negative control for the *mtsfgFP* (*mtNptII*) gene fragment, followed by lane 9, showing its amplified product at 809 bp. Lane 10 contained a 100 bp DNA ladder. The distinct bands shown in the amplified lanes prove the successful and specific amplification of the targeted gene fragments under the applied PCR conditions.

4.3.3 Quantification of purified product

The amplified *NptII*, *^{mt}NptII* and *^{mt}sfGFP* gene products were purified using an EZ-10 Spin Column DNA Gel Extraction Kit. Table 4.1 shows the concentration and purity of the purified PCR product, measured using a NanoDrop spectrophotometer.

Table 4.1: Concentrations and purities of purified *NptII*, *^{mt}NptII* and *^{mt}sfGFP* fragments.

Purified PCR product	Concentration (ng/ μ L)	Primary purity (A260/A280)	Secondary purity (A260/A230)
<i>NptII</i> gene fragment	82.3	1.88	2.20
<i>^{mt}NptII</i> gene fragment	105.9	1.85	2.20
<i>^{mt}sfGFP</i> (<i>NptII</i>) gene fragment	60.3	1.85	2.19
<i>^{mt}sfGFP</i> (<i>^{mt}NptII</i>) gene fragment	176.3	1.85	2.23

4.4 Overlap extension PCR for construct *NptII*-*mtsfGFP* and *mtNptII*-*mtsfGFP* fusion gene

4.4.1 *NptII*-*mtsfGFP* and *mtNptII*-*mtsfGFP* fusion gene

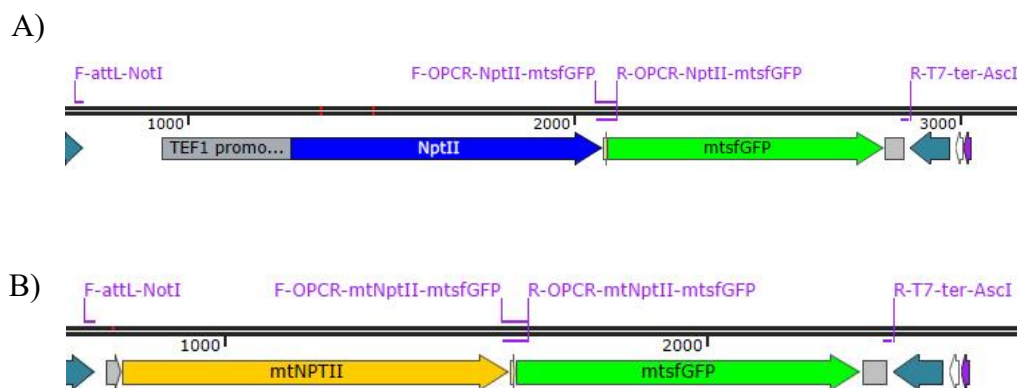


Figure 4.6: Schematic showing the sequence of the construction of the *NptII*-*mtsfGFP* and *mtNptII*-*mtsfGFP* fusion genes. In part A, the *NptII*-*mtsfGFP* was fused by the overhanging regions, whole fusion gene sequences were amplified by end-to-end primers which is F-attL-NotI and R-T7-Ter-AscI. In part B, *mtNptII*-*mtsfGFP* was also fused by the overhanging regions, whole fusion gene sequences were amplified by end-to-end primers which is F-attL-NotI and R-T7-Ter-AscI.

4.4.2 Result of agarose gel electrophoresis

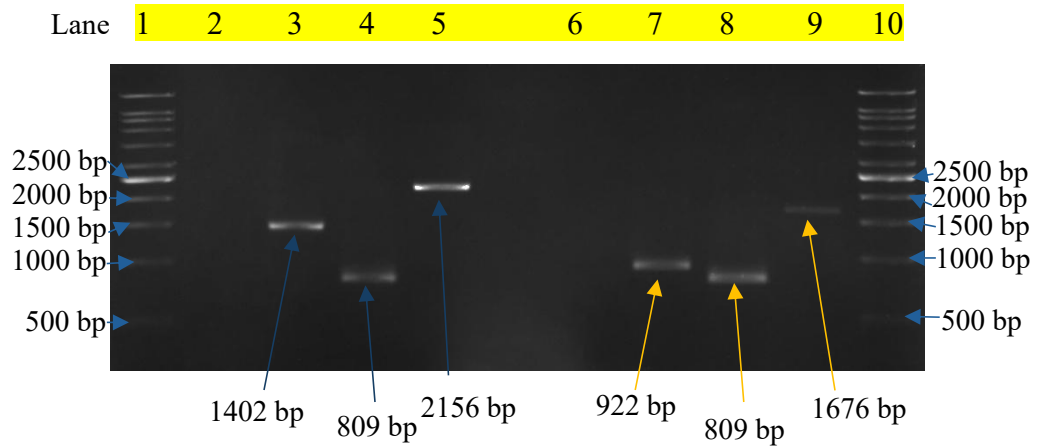


Figure 4.7: Overlap extension PCR for *NptII-mtsGFP* and *mtsNptII-mtsGFP* fusion genes electrophoresed on 0.8% (w/v) agarose gel. Lane 1 contains the 100 bp DNA ladder as a molecular weight marker, and lane 2 contains the negative control for the *NptII-mtsGFP* fusion gene. Lanes 3 and 4 show positive controls for the *NptII* gene fragment (1402 bp) and *mtsGFP(NptII)* gene fragments (809 bp), respectively. Lane 5 shows the amplified *NptII-mtsGFP* fusion gene product at 2156 bp. Lane 6 contains the negative control for the *mtsNptII-mtsGFP* fusion gene; at the same time, lanes 7 and 8 show the positive controls for the *mtsNptII* gene fragment (922 bp) and *mtsGFP (mtsNptII)* gene fragment (809 bp) accordingly. Lane 9 shows the successfully amplified *mtsNptII-mtsGFP* fusion gene at 1676 bp, while lane 10 contained the 1 kb DNA ladder. The presence of single, clearly fused gene bands in lanes 5 and 9 proves the successful and specific fusion under the optimized overlap extension PCR conditions, with the absence of amplification in negative controls.

4.4.3 Quantification of purified product

Two PCR fusion gene products were purified using different methodologies for DNA sequencing. *NptII-^{mt}sfGFP* fusion gene product was purified using an EZ-10 Spin Column DNA Gel Extraction Kit. To reduce DNA loss during gel electrophoresis, ethanol precipitation was used to purify the *^{mt}NptII-^{mt}sfGFP* fusion gene product. Table 4.2 shows the concentration and purity of the purified PCR product measured using a NanoDrop spectrophotometer.

Table 4.2: Concentrations and purities of purified *NptII-^{mt}sfGFP* and *^{mt}NptII-^{mt}sfGFP* fusion genes.

Purified PCR product	Concentration (ng/ μ L)	Primary purity (A260/A280)	Secondary purity (A260/A230)
<i>NptII-^{mt}sfGFP</i> fusion gene	109.7	1.86	2.16
<i>^{mt}NptII-^{mt}sfGFP</i> fusion gene	624.7	1.41	1.82

4.5 Verification of the fusion gene product by DNA sequencing

The *NptII*-*mtsfGFP* fusion gene product was successfully verified by DNA sequencing. The results were analyzed with the *NptII* and *mtsfGFP* gene fragments, which were already verified by DNA sequencing by BLASTN. The alignment sequences are displayed in Appendices E and G.

CHAPTER 5

DISCUSSION

5.1 Justification for using overlap extension PCR in generate the fusion gene construction

In this project, overlap extension PCR (OE-PCR) was utilized to construct the *NptII^{-mt}sfGFP* and *^{mt}NptII-sfGFP* fusion gene constructs. Using custom-made overlapping primers, OE-PCR enables the precise and seamless fusion of two or more DNA fragments by creating the complementary overlap regions between the target genes (Bryksin and Matsumura, 2010). This method provides a highly specific fusion junction that remains in the open reading frame of the target fusion gene without adding unwanted sequences such as restriction enzyme recognition sites or linker residues (Hilgarth and Lanigan, 2020).

Compared with the traditional restriction enzyme-based cloning method, OE-PCR has significant advantages. Restriction enzyme cloning is highly dependent on the availability of suitable restriction sites in the vector and the insertion of DNA. This requires the introduction of an extra sequence that may affect protein function, without suitable restriction sites (Hashemabadi *et al.*, 2025). In addition, multiple labor-intensive steps were included in the

restriction enzyme cloning such as digestion with restriction enzymes, fragment purification, ligation, and screening with colony PCR. The whole process requires several days and is costly, especially when rare restriction enzymes are chosen.

In contrast, OE-PCR is more rapid and cost-effective, without the need for preexisting or engineered restriction sites. Only three rounds of PCR are required for OE-PCR, including the individual fragment amplification and fusion step. Without the requirement of restriction sites, OE-PCR is highly versatile, allowing seamless joining of any DNA fragment by designing overlapping primers. Moreover, the linearized fusion product can also be directly cloned into the plasmid through recombination methods (Nelson and Fitch, 2012), thereby simplifying further workflow.

Furthermore, the troubleshooting of OE-PCR has focused on optimizing the PCR conditions and primer design; these issues are often straightforward to address. In comparison, restriction enzyme cloning method is more challenging due to multiple problems such as incomplete digestion or inefficient ligation, which are more difficult and time-consuming to resolve (Makam *et al.*, 2018). Therefore, these factors led the selection of OE-PCR as the preferred method for construct *NptII^{mt}NptII^{mt}sfGFP* fusion gene.

5.2 Megaprimer design

To generate the *NptII^{mt}NptII^{mt}sfGFP* fusion gene by OE-PCR, overlapping regions were designed between the two DNA fragments, allowing them to serve as primers for each other in subsequent reactions using fragments with complementary overlapping ends. Megaprimers include overlapping sequences and target fragment sequences to facilitate gene fusion with specific binding and extension steps.

One of the most important design features of OE-PCR is that only the second gene fragment contains a stop codon (Hilgarth and Lanigan, 2020). By removing the stop codon in the first fusion gene fragment, the polymerase allowed to fully extend the overlap region without premature dissociation and incomplete fusion.

In this project, megaprimers with a length of 55 bp were designed to carry overlapping regions. Longer than the 18-24 bp typical primer. The increased length of the primer increases the melting temperature (T_m) and enhances binding specificity, providing sufficient homology to minimize nonspecific binding and increase the annealing specificity. According to Tyagi, Lai, and Duggleby (2004), some megaprimers exceeded 300 bp in some OE-PCR applications; therefore, the primer length is not strictly limiting, but good hybridization and extension need to be ensured to maximize fusion efficiency. The basis of the megaprimer is to contain the overlapping region between two

gene fragments and be long enough to generate a higher-specificity overlap region for further overlapping steps.

5.3 Challenges in single-primer testing

In figure 4.2, all megaprimers in this project were prone to secondary structure formation, including hairpin formation and self-annealing from the Oligonucleotide Properties Calculator analysis. The increased length of the megaprimer increases the possibility of an intramolecular secondary structure because of inverted repeats with a higher occurrence rate. These secondary structures can hinder the proper annealing of the target DNA and cause premature termination or reduce the efficiency of DNA polymerase extension (Hilgarth and Lanigan, 2020). Additionally, another potential problem reducing the amplification specificity is primer-dimer formation.

During single-primer testing with the corresponding DNA template, target-sized bands were clearly observed on agarose gel. This is the most significant issue and reveals a risk of false positives because there is a fake band at the target size. Hence, the main function of single-primer testing is to modify the PCR conditions until the fake bands disappear for further steps.

To mitigate these issues, the PCR conditions were modified step-by-step. The annealing temperatures were initially calculated using the Vayzme T_m calculator and optimized as required because of the high T_m ($\sim 69^\circ\text{C}$) of the

megaprimers. Annealing temperatures above 60°C yielded cleaner products but lower overall amplification efficiency. This makes the purification challenging. Thus, a suitable annealing temperature to compromise between specificity and yield was determined using PCR (Forloni, Liu and Wajapeyee, 2019).

The number of PCR thermocycles was optimized. Excessive cycles increase non-specific amplification and mutation rates. For most fragments, cycling was reduced from 35 to 25 cycles to eliminate false-positive results in single primer testing. Some cases need to be reduced to 20 cycles. The most challenging problem in cycling-number optimization is the comparison of the balance between productivity and specificity in the PCR amplification step.

The addition of DMSO was tested to destabilize the secondary structure by weakening the hydrogen bonds between complementary base pairs. The addition of DMSO to the PCR mixture effectively reduced non-specific amplification (Varadharajan and Parani, 2021) and interfered with target amplification in the later stages. Although T_m was lowered, the target PCR product could not be formed properly due to the presence of DMSO.

Then, based on the previous adjustment, the concentration of primer in the PCR mixture was reduced from 0.5 μM to 0.3 μM . Primer-dimer formation and non-specific amplification were successfully minimized, except for the *NptII* gene fragment, which required further adjustment of the cycling number to achieve a clean band.

This part required substantial time and repeated adjustments before moving forward. Although sometimes the results of single-primer testing yielded clean agarose gel without any band formation, the modified parameter often caused a significant drop in PCR product yield. The low concentration of DNA makes purification challenging. Hence, the PCR product must be reduced because the concentration of the DNA template is less than a certain level. In addition, resolving this balance between specificity and yield was challenging with the modification of the annealing temperature, primer concentration, thermocycling number, and additives. This iterative process is time-consuming and laborious, indicating that high specificity does not guarantee smooth downstream amplification and purification.

5.4 Amplification of the target gene fragments

Based on the PCR conditions modified by single-primer testing, each gene fragment was amplified with the appropriate primer pairs listed in Tables 3.1, 3.2, and 3.3. Modifications to the thermocycling parameters and PCR mixtures were necessary for several fragments. except for the *mtsfGFP* gene fragment that fused to *NptII*, which required only a few adjustments.

For the *NptII* gene fragment, the significant differences in T_m between the forward (54.8°C) and reverse primers (66.2°C) resulted in a higher annealing temperature (58°C). This is the maximum annealing temperature with the target band size after PCR testing to balance specificity and yield. Thus, annealing

temperatures of 56°C and 58°C were maintained as a compromise between the specificity and yield. In this case, both PCR products showed nonspecific amplicons; thus, a lower annealing temperature was chosen. Based on the data from single-primer testing and further PCR condition modification, a light band was observed on the agarose gel. Although the target band was successfully obtained, the low DNA concentration product required re-amplification using the PCR product as the template.

mtNptII gene fragment amplification was similar to *NptII* optimization with an annealing temperature of approximately 56°C by a series of gradient PCR tests. In contrast, the annealing temperature of the *mtsfGFP* gene fragment containing the *mtNptII* gene overlap region was approximately 60°C, without reducing the amplicon concentration and non-specific appearance. Because the concentration of the target DNA product was drastically reduced by the gel purification kit, the *mtsfGFP* gene fragment was reamplified using the purified product as the DNA template.

The elongation time was set according to the length of the gene fragment and efficiency of the Vayzme *Taq* polymerase. With 1 min per 1 kb DNA synthesis extension speed recommendation, 1:30 min for the *NptII* gene fragment and other gene fragments below 1 kb only required 1 min to synthesize.

5.5 Overlap extension PCR

The final OE-PCR step fused the purified individual gene fragments containing overlapping regions to construct the full-length *NptII-^{mt}sfGFP* and *^{mt}NptII-sfGFP* fusion genes. Before the fusion step, the PCR products were purified to remove salts, enzymes, and buffers that may inhibit further reactions, and the concentration was measured by NanoDrop spectrophotometry.

Although the input DNA ratio for fusion was initially calculated using bioinformatics tools, such as the Vayzme Input DNA calculator (<https://www.vazymeglobal.com/cetool/restructure.html>), empirical modifications are still required based on product quality. The primary challenge was non-specific bands, which can be caused by suboptimal PCR conditions, including lower annealing temperature, excessive cycle number, or primers with sequence complementarity, leading to self- or cross-annealing problems.

To solve this problem, the PCR conditions and the ratio of the input DNA were modified. The annealing temperature for the fusion reactions was set to match the T_m of the overlap region. Fusion without primers at 60°C showed adequate annealing but may have reduced the efficiency; therefore, the temperature was carefully optimized. Although in single primer testing, the primer will not anneal with the template, in end-to-end PCR amplification, the primer may anneal with the residual template fragments and cause non-specific amplification. Based on this hypothesis, the DNA ratio was modified. The amount of the longer gene fragment in the fusion gene decreased, whereas the shorter gene fragment remained. The results showed that it efficiently reduced the non-specific bands, especially the residual template fragments. In end-to-

end PCR amplification with external primers followed by fusion, the annealing temperatures were chosen as 59°C for the *NptII-mt⁺sfGFP* fusion gene and 60°C for the *mtNptII-mt⁺sfGFP* fusion gene in the balance between yield and specificity to reduce nonspecific products.

5.6 Purification of *NptII-mt⁺sfGFP* and *mtNptII-mt⁺sfGFP* fusion genes products

Two strategies were used to purify the fusion gene products. Ethanol precipitation was preferred for the *mtNptII-mt⁺sfGFP* fusion gene to minimize DNA loss compared with gel extraction, especially with the faint amplification band. In the absence of agarose gel electrophoresis, the DNA content of the PCR products was preserved.

To send the sequencing to 1st BASE, the quality of the DNA concentrations required exceeded 30 ng/μL for fragments longer than 1500 bp. The *NptII-mt⁺sfGFP* fusion gene met this requirement, whereas *mtNptII-mt⁺sfGFP* did not result from gel residue contamination. The residual agarose gel in the phenol-chloroform-isoamyl alcohol supernatant extraction step led to a lower purity of the *mtNptII-mt⁺sfGFP* fusion gene product. This problem can be eliminated by repeating this extraction step until the buffy coat between the supernatant and phenol-chloroform-isoamyl alcohol is clear. This action maximizes DNA separation from the melting agarose gel.

5.7 DNA sequencing

Sequencing of the *NptII-mt^{sf}GFP* fusion gene product confirmed the successful fusion gene construction. The alignment results that matched the control sequence were confirmed by a senior. Owing to insufficient purity, sequencing of the *mtNptII-mt^{sf}GFP* fusion gene product was not feasible. Instead, it was cloned into *E. coli* and sequenced after plasmid extraction for correct fusion. The sequencing data and alignments are provided in the Appendix C.

5.8 The fusion pf selectable marker and reporter gene

In previous human cell studies, selectable marker and reporter fusion genes have been constructed. The green fluorescent protein (GFP) was successfully fused with the *neomycin* (*Neo*) resistance gene (Zhang, 2014). This study successfully overcame the common challenges in maintaining both gene functions by simple in-frame linking, without causing misfiling or steric hindrance. The native *GFP* stop codon was removed, enabling fusion with *Neo*, and the fusion genes were initiated by a mutated start codon. Approximately 17 amino acid linkers were inserted between the fusion genes to ensure the proper folding and activity of both protein domains. Through fusion gene testing, the researchers found that the fusion gene products exhibited green fluorescence 30% better than wild-type GFP, while the *Neo* function still retained resistance to aminoglycoside antibiotics. With a specific targeting sequence, the synthesis protein generated by the nucleus is transferred and functions in the mitochondria of the host. In related studies, GFP-*Neo* proteins, which fuse with the mitochondrial targeting leader sequence from mouse mitochondrial

transcription factor A, were able to target and localize inside the mitochondrial matrix of human cells (HeLa cells) (Yoon and Koob, 2008). This functional fusion protein proves that the fusion of the selectable marker and reporter gene is available and the localization can be confirmed by fluorescence microscopy and biochemical fractionation while maintaining the antibiotic resistance within mitochondria and showing mitochondrial network co-localization without cytosolic presence.

In studies of the *^{mt}NptII* gene, researchers fused it with mitochondrial targeting sequences (MTS), which are derived from mitochondrial proteins and allow the import of the fusion protein from the cytosol into the mitochondria. The synthesis protein can be expressed in mitochondria (Boob et al., 2024). The specific localization of *^{mt}NptII* was confirmed using fluorescence microscopy and biochemical fractionation.

Based on both studies, we discovered that the fusion of the selective markers and reporter genes is possible with proper folding and undergoes the function. In addition, the modified *^{mt}NptII* can be expressed inside the host cell mitochondria using MTS. Thus, we planned to construct the *NptII/^{mt}NptII-^{mt}sfGFP* fusion gene product based on this concept.

5.8.1 Advantages of selectable marker and reporter fusion genes

In this study, *^{mt}NptII* genes served as dual-function genes. As an antibiotic resistance gene, it is possible to select transformed plasmids from non-

transformed plasmids. In addition, it serves as a transgene. Typically, the GOI is tagged with GFP to visualize its expression and level. In this project, *mtNptII* replaced the GOI and fused the *mtsfGFP* gene inside the pENTR cassette. With the engineered AMT system, which is able to transfer the GOI to integrate and express the host's mitochondria, it is able to generate functional genes. When the GOI is replaced by *mtNptII* and expressed inside the host's mitochondria, it can be visualized inside the host cell through fluorescence microscopy due to the criteria of subcellular localization. In addition, the synthesized protein can be verified using an anti-GFP tag to detect GFP with its fusion gene. Based on these methods, quantitative and qualitative methods were used. For example, we can observe that the result in the selectable medium is qualitative, and now quantitative is used to detect the fluorescent intensity. Through both sets of obtained data, we can eliminate the false positive result that is caused by the auxochrome of some host cells.

5.8.2 Disadvantages of selectable marker and reporter fusion genes

Due to the *NptII/mtNptII-mtsfGFP* fusion gene, larger proteins require longer mRNA transcripts, increasing the energetic need and slowing down the transcriptional process. Similar to the translational process, longer mRNA require more time and resources to translate into proteins. Thus, larger fusion genes will decrease expression levels compared to smaller proteins (Lopes *et al.*, 2021; Lemos, 2005).

In addition, larger proteins often have complex tertiary structures, creating a challenge for folding efficiency, and the misfolding or aggregation rate increases. Improper folding causes misfolded proteins to be degraded by the cellular quality control mechanism to reduce their net expression level (Lemos, 2005).

5.9 Trouble shooting

Secondary structures such as hairpin formation and primer dimers in PCR reactions decrease the amplification efficiency and cause non-specific bands to appear in the results. These structures were observed when the complementary primer sequences were self-annealing intramolecular or intermolecular. One effective method to solve this problem is to replace amino acids, which are encoded by problematic DNA sequences. These secondary structures can be removed by changing the nucleotide composition of megaprimers while maintaining protein function. For instance, the codons GAA and GAG encode the same amino acid glutamic acid. By substituting amino acids without changing the properties of the protein, the secondary structure can be destabilized and removed. Moreover, compared to chemical additives, such as DMSO, conservative amino acid substitutions provide a molecular solution to the problem beyond chemical mitigation (Bohórquez, Suárez and Patarroyo, 2017).

In addition, without modifying the megaprimers, we could increase the specificity of the primer in the PCR reaction. Before using the megaprimers to amplify each gene fragment, the DNA template was amplified using typical

primers. First, the gene fragments were amplified with normal primers to increase the specificity of the primer, and the PCR products were used as the DNA template with megaprimers containing the overhanging regions. Using the target gene fragments, PCR products as the DNA template instead of the original DNA fragments, increases the specificity of megaprimers and decreases the chance of forming secondary structures. This approach increases the rate of occurrence of specific band formation.

Furthermore, it is easier to construct fusion genes using traditional restriction enzyme methods. Due to the higher secondary structure formation rate using OE-PCR, using a restriction enzyme to recombine the target genes is a way to overcome this problem. In megaprimer design, we can add a linker between the two fusion genes. This linker includes the desired recognition sites, allowing the fusion of two genes using the traditional restriction enzyme method if OE-PCR fails. This method can reduce the time required to modify the optimum PCR reaction parameters based on these studies to remove secondary structures.

In summary, using synonymous codon changes in megaprimers, using target gene PCR products as the DNA template in the first amplification with megaprimers, and changing the fusion methods to restriction enzyme methods overcomes the secondary structure formation in PCR reactions.

5.10 Further studies

This project successfully fused two gene fragments using OE-PCR to create a dual-function fusion gene plasmid. The *NptII* gene serves as a selectable marker and is able to resist antibiotics, such as kanamycin and neomycin (Numata *et al.*, 2016). The *^{mt}NptII* gene is modified for mitochondrial DNA expression compatibility. The *^{mt}sfGFP* gene acts as a reporter gene, emitting green fluorescence that allows visualization of protein localization and dynamics inside the mitochondria (Yap,2025).

The fusion gene plasmid enables the selection of host cells and allows direct observation of the expressed fusion protein, thereby facilitating gene functional studies (Zhao *et al.*, 2011). This construct can be cloned into an expression vector and transformed in yeast using a yeast-two-hybrid assay, aiding in interaction mapping and functional characterization. Finally, it can be transferred into agrobacteria using the yeast-two hybrid method to infect the target plant and perform functional gene studies. From this *^{mt}NptII-^{mt}sfGFP* fusion gene construct, the GOI, which is targeted to be expressed in the host's mitochondria, can be proven by observing protein synthesis and remaining inside the mitochondria by green fluorescence under UV or blue light.

CHAPTER 6

CONCLUSION

The purpose of this project was to fuse two sets of gene fragments to generate the *NptII-mt⁺sfGFP* and *mt⁺NptII-mt⁺sfGFP* fusion genes. Both fusion products were successfully verified by DNA sequencing, proving the project's aim. In this project, overlap extension PCR (OE-PCR) enabled precise and seamless fusion of DNA fragments through custom-designed overlapping primers and proper protocols. Compared to traditional restriction enzyme cloning, which requires multiple labor-intensive steps, such as digestion, ligation, and screening, OE-PCR condenses the process into a few PCR reactions. This technique reduces the time, cost, and simplicity of the workflow, while maintaining high specificity. However, the length of the megaprimers contributed to challenges, including secondary structure formation and single-primer amplification. Hence, single-primer testing was essential to prove critical in eliminating false positive results and to preliminarily optimize PCR reaction conditions. Parameters such as annealing temperature, primer concentration, cycle number, and additives such as DMSO make it difficult for the single primer to anneal to the template. For gene fragment amplification, PCR conditions were modified to accommodate differences in primer melting temperatures and template complexity. This balance was crucial in the specificity and amplification yield; increasing the specificity tended to complicate the subsequent purification step.

NptII (1402 bp), *^{mt}NptII* (922 bp), and *^{mt}sfGFP* (802 bp) gene fragments with overlapping regions were successfully amplified. Subsequent fusion and final amplification steps amplified the *NptII-^{mt}sfGFP* (2156 bp) and *^{mt}NptII-^{mt}sfGFP* (1676 bp) fusion gene products by modifying the PCR conditions. Different purification methods were used to maximize DNA recovery, despite the low yield in different cases. Successful assembly of fusion gene products was verified by gel electrophoresis and DNA sequencing. The fusion gene product was cloned into *E. coli* by a senior lab member, and the selectable marker and reporter gene functions were combined into a plasmid. This dual-function plasmid is a valuable tool for future functional genetic studies. Lastly, this project highlights the essential role of the primer design and PCR condition optimization in achieving fusion gene construction by OE-PCR with technical demands.

REFERENCES

- Andrews, B.T. *et al.* (2007) ‘The rough energy landscape of superfolder GFP is linked to the chromophore’, *Journal of Molecular Biology*, 373(2), pp. 476–490. Available at: <https://doi.org/10.1016/j.jmb.2007.07.071>.
- Boob, A.G. *et al.* (2024) ‘Design of diverse, functional mitochondrial targeting sequences across eukaryotic organisms using variational autoencoder’, *bioRxiv (Cold Spring Harbor Laboratory)*. Available at: <https://doi.org/10.1101/2024.08.28.610205>.
- Barondeau, D.P. *et al.* (2003) ‘Mechanism and energetics of green fluorescent protein chromophore synthesis revealed by trapped intermediate structures’, *Proceedings of the National Academy of Sciences*, 100(21), pp. 12111–12116. Available at: <https://doi.org/10.1073/pnas.2133463100>.
- Barton, K.A. *et al.* (1983) ‘Regeneration of intact tobacco plants containing full length copies of genetically engineered T-DNA, and transmission of T-DNA to R1 progeny’, *Cell*, 32(4), pp. 1033–1043. Available at: [https://doi.org/10.1016/0092-8674\(83\)90288-x](https://doi.org/10.1016/0092-8674(83)90288-x).
- Becker, D. *et al.* (1992) ‘New plant binary vectors with selectable markers located proximal to the left T-DNA border’, *Plant Molecular Biology*, 20(6), pp. 1195–1197. Available at: <https://doi.org/10.1007/bf00028908>.
- Bernard, P. (1996) ‘Positive selection of recombinant DNA by ccdB’, *BioTechniques*, 21(2), pp. 320–323. Available at: <https://doi.org/10.2144/96212pf01>.
- Bohórquez, H.J., Suárez, C.F. and Patarroyo, M.E. (2017) ‘Mass & secondary structure propensity of amino acids explain their mutability and evolutionary replacements’, *Scientific Reports*, 7(1). Available at: <https://doi.org/10.1038/s41598-017-08041-7>.
- Bourras, S., Rouxel, T. and Meyer, M. (2015) ‘*Agrobacterium tumefaciens* gene transfer: how a plant pathogen hacks the nuclei of plant and nonplant organisms’, *Phytopathology*, 105(10), pp. 1288–1301. Available at: <https://doi.org/10.1094/phyto-12-14-0380-rvw>.

Bryksin, A. and Matsumura, I. (2010) 'Overlap extension PCR cloning: a simple and reliable way to create recombinant plasmids', *BioTechniques*, 48(6), pp. 463–465. Available at: <https://doi.org/10.2144/000113418>.

Chang, S. *et al.* (2025) 'Malaysian journal of microbiology published by malaysian society for microbiology a vir binary vector system for *Agrobacterium*-mediated transient transformation in *Nicotiana benthamiana*', *Malaysian Journal of Microbiology*, 21(2). Available at: <https://doi.org/10.21161/mjm.240632>.

Curtis, M.D. and Grossniklaus, U. (2003) 'A gateway cloning vector set for high-throughput functional analysis of genes in planta', *Plant Physiology*, 133(2), pp. 462–469. Available at: <https://doi.org/10.1104/pp.103.027979>.

Das, A. *et al.* (2020) 'Estimation of *neomycin phosphotransferase-II (NptII)* protein in vegetative and reproductive tissues of transgenic chickpea (*Cicer arietinum* L.) and biosafety perspectives', *Journal of Plant Biochemistry and Biotechnology*, 29(3), pp. 568–570. Available at: <https://doi.org/10.1007/s13562-020-00562-z>.

De Saeger, J. *et al.* (2021) '*Agrobacterium* strains and strain improvement: Present and outlook', *Biotechnology Advances*, 53, p.107677. Available at: <https://doi.org/10.1016/j.biotechadv.2020.107677>.

Forloni, M., Liu, A.Y. and Wajapeyee, N. (2019) 'Megaprimer polymerase chain reaction (PCR)-based mutagenesis', *Cold Spring Harbor Protocols*, 2019(6), p.097824. Available at: <https://doi.org/10.1101/pdb.prot097824>.

Gelvin, S.B. (2003) '*Agrobacterium*-Mediated plant transformation: the biology behind the “gene-jockeying” tool', *Microbiology and Molecular Biology Reviews*, 67(1), pp. 16–37. Available at: <https://doi.org/10.1128/mmbr.67.1.16-37.2003>.

Hashemabadi, M. *et al.* (2025) 'Restriction enzyme-free method for generating PCR product sticky ends in recombinant vector construction for cloning', *Discover Applied Sciences*, 7(5). Available at: <https://doi.org/10.1007/s42452-025-06770-3>.

Hilgarth, R.S. and Lanigan, T.M. (2020) 'Optimization of overlap extension PCR for efficient transgene construction', *MethodsX*, 7, p. 100759. Available at: <https://doi.org/10.1016/j.mex.2019.12.001>.

Hsu, S.-T.D., Blaser, G. and Jackson, S.E. (2009) 'The folding, stability and conformational dynamics of β -barrel fluorescent proteins', *Chemical Society Reviews*, 38(10), p. 2951. Available at: <https://doi.org/10.1039/b908170b>.

Hwang, H.-H., Yu, M. and Lai, E.-M. (2017) 'Agrobacterium-mediated plant transformation: biology and applications', *The Arabidopsis Book*, 15(15), p. e0186. Available at: <https://doi.org/10.1199/tab.0186>.

Karimi, M., Depicker, A. and Hilson, P. (2007) 'Recombinational cloning with plant gateway vectors', *Plant Physiology*, 145(4), pp. 1144–1154. Available at: <https://doi.org/10.1104/pp.107.106989>.

Karimi, M., Inzé, D. and Depicker, A. (2002) 'GATEWAY™ vectors for Agrobacterium-mediated plant transformation', *Trends in Plant Science*, 7(5), pp. 193–195. Available at: [https://doi.org/10.1016/s1360-1385\(02\)02251-3](https://doi.org/10.1016/s1360-1385(02)02251-3).

Kumar, A. and Pal, D. (2016) 'Green fluorescent protein and their applications in advance research', *Journal of Research in Engineering and Applied Sciences*, 01(01), pp. 42–46. Available at: <https://doi.org/10.46565/jreas.2016.v01i01.007>.

Kumar, A.U. and Ling, A.P.K. (2021) 'Gene introduction approaches in chloroplast transformation and its applications', *Journal of Genetic Engineering and Biotechnology*, 19(1). Available at: <https://doi.org/10.1186/s43141-021-00255-7>.

Law, S.S.Y. *et al.* (2022) 'Polymer-coated carbon nanotube hybrids with functional peptides for gene delivery into plant mitochondria', *Nature Communications*, 13(1), p. 2417. Available at: <https://doi.org/10.1038/s41467-022-30185-y>.

Lemos, B. (2005) 'Evolution of proteins and gene expression levels are coupled in *Drosophila* and are independently associated with mRNA abundance, protein length, and number of protein-protein interactions', *Molecular Biology and Evolution*, 22(5), pp. 1345–1354. Available at: <https://doi.org/10.1093/molbev/msi122>.

Lopes, I. *et al.* (2021) 'Gene size matters: an analysis of gene length in the human genome', *Frontiers in Genetics*, 12. Available at: <https://doi.org/10.3389/fgene.2021.559998>.

Lund, B.A., Leiros, H.-K.S. and Bjerga, G.K. (2014) 'A high-throughput, restriction-free cloning and screening strategy based on *ccdB* gene replacement,' *Microbial Cell Factories*, 13(1). <https://doi.org/10.1186/1475-2859-13-38>.

Makam, S. *et al.* (2018) 'An efficient method for integration of PCR fragments into adjacent or overlapping restriction sites during gene cloning', 3 *Biotech*, 8(4), p. 197. Available at: <https://doi.org/10.1007/s13205-018-1214-2>.

Miki, B. and McHugh, S. (2004) 'Selectable marker genes in transgenic plants: applications, alternatives and biosafety', *Journal of Biotechnology*, 107(3), pp. 193–232. Available at: <https://doi.org/10.1016/j.jbiotec.2003.10.011>.

Mosey, M. *et al.* (2021) 'Methodological review of genetic engineering approaches for non-model algae', *Algal Research*, 54, p. 102221. Available at: <https://doi.org/10.1016/j.algal.2021.102221>.

Munaweera, T.I.K. *et al.* (2022) 'Modern plant biotechnology as a strategy in addressing climate change and attaining food security', *Agriculture & Food Security*, 11(1). Available at: <https://doi.org/10.1186/s40066-022-00369-2>.

Nelson, M.N. and David (2011) 'Overlap Extension PCR: an efficient method for transgene construction', *Methods in Molecular Biology*, pp. 459–470. Available at: https://doi.org/10.1007/978-1-61779-228-1_27.

Numata, K. *et al.* (2016) 'Direct introduction of *neomycin phosphotransferase* II protein into apple leaves to confer kanamycin resistance', *Plant Biotechnology*, 33(5), pp. 403–407. Available at: <https://doi.org/10.5511/plantbiotechnology.16.0929a>.

Orm , M. *et al.* (1996) 'Crystal structure of the *Aequorea victoria* green fluorescent protein', *Science*, 273(5280), pp. 1392–1395. Available at: <https://doi.org/10.1126/science.273.5280.1392>.

Pedelacq, J.-D. and Cabantous, S. (2019) 'Development and applications of superfolder and split fluorescent protein detection systems in biology', *International Journal of Molecular Sciences*, 20(14), p. 3479. Available at: <https://doi.org/10.3390/ijms20143479>.

Reece-Hoyes, J.S. and Walhout, A.J.M. (2018) 'Propagating gateway vectors', *Cold Spring Harbor Protocols*, 2018(1), p. pdb.prot094920. Available at: <https://doi.org/10.1101/pdb.prot094920>.

Soboleski, M.R., Oaks, J. and Halford, W.P. (2005) 'Green fluorescent protein is a quantitative reporter of gene expression in individual eukaryotic cells', *The FASEB Journal*, 19(3), pp. 440–442. Available at: <https://doi.org/10.1096/fj.04-3180fje>.

Strathdee, C.A., McLeod, M.R. and Underhill, T.M. (2000) 'Dominant positive and negative selection using luciferase, green fluorescent protein and B-Galactosidase Reporter gene fusions,' *BioTechniques*, 28(2), pp. 210–214. <https://doi.org/10.2144/00282bm04>.

Tyagi, R., Lai, R. and Duggleby, R.G. (2004) 'A new approach to “megaprimer” polymerase chain reaction mutagenesis without an intermediate gel purification step', *BMC Biotechnology*, 4(1), p. 2. Available at: <https://doi.org/10.1186/1472-6750-4-2>.

Tzfira, T. and Citovsky, V. (2008) *Agrobacterium: From Biology to Biotechnology*. Edited by T. Tzfira and V. Citovsky. New York, NY: Springer New York. Available at: <https://doi.org/10.1007/978-0-387-72290-0>.

Varadharajan, B. and Parani, M. (2021) 'DMSO and betaine significantly enhance the PCR amplification of ITS2 DNA barcodes from plants', *Genome*. Edited by J.S. Boatwright, 64(3), pp. 165–171. Available at: <https://doi.org/10.1139/gen-2019-0221>.

Wiese, M. and Bannister, A.J. (2020) 'Two genomes one cell: mitochondrial-nuclear coordination via epigenetic pathways', *Molecular Metabolism*, 38. Available at: <https://doi.org/10.1016/j.molmet.2020.01.006>.

Yap.K.H. (2025) *Construction of agrobacterium vector systems for nuclear and mitochondrial transformation in yeast*. Master thesis. Universiti Tunku Abdul Rahman.

Yoon, Y.G. and Koob, M.D. (2008) 'Selection by drug resistance proteins located in the mitochondria of mammalian cells', *Mitochondrion*, 8(5-6), pp. 345–351. Available at: <https://doi.org/10.1016/j.mito.2008.07.004>.

Zhang, M.L.J. (2014) 'Construction of functional *GFP-Neo* fusion protein by selection from a peptide library,' *Cloning & Transgenesis*, 03(03). <https://doi.org/10.4172/2168-9849.1000131>.

Zhao, H. *et al.* (2011) 'Fusion gene vectors allowing for simultaneous drug selection, cell labeling, and reporter assay in vitro and in vivo', *Analytical Chemistry*, 84(2), pp. 987–993. Available at: <https://doi.org/10.1021/ac202541t>.

Appendix A

Table A: The list of chemicals, reagents, and kits used in this final year project with their corresponding manufactures.

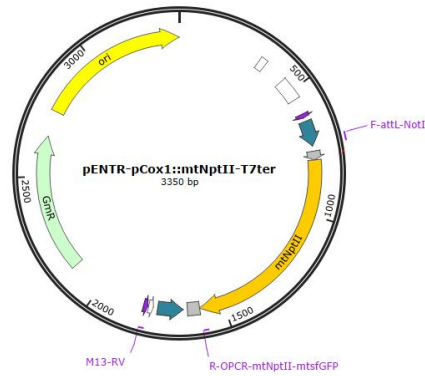
Chemicals	Manufacturers
100 bp DNA ladder	Norgen Biotek Corp.
100 % ethanol	CIM
2 x Taq master mix	Vazyme
Agarose	1 st BASE Pte Ltd
Boric acid	Chemos
Low-melting agarose	BM Bio
Sodium chloride	Chem Soln
DyeAll™ staining solution	Gene All
Ethylenediaminetetraacetic (EDTA)	SIME Scientific
EZ-10 Spin Column DNA Gel Extraction Kit	Bio Basic Canada Inc.
Glacial acetic acid	Sigma-Aldrich
Phenol-chloroform-isoamyl alcohol	Nacalai Tesque Inc.
Sodium acetate (NaOAc)	Sigma-Aldrich
Tris base	Vivantis

VC 1 kb DNA ladder

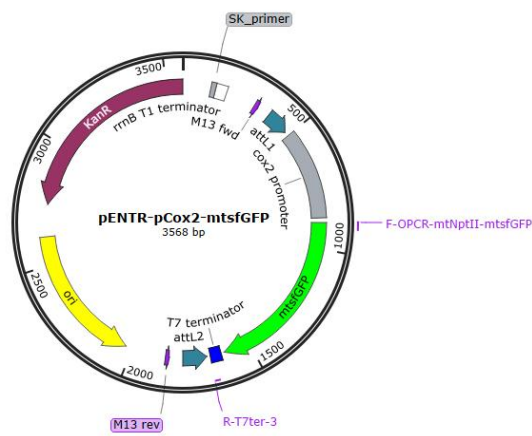
Vivantis

Appendix B

A



B)



C)

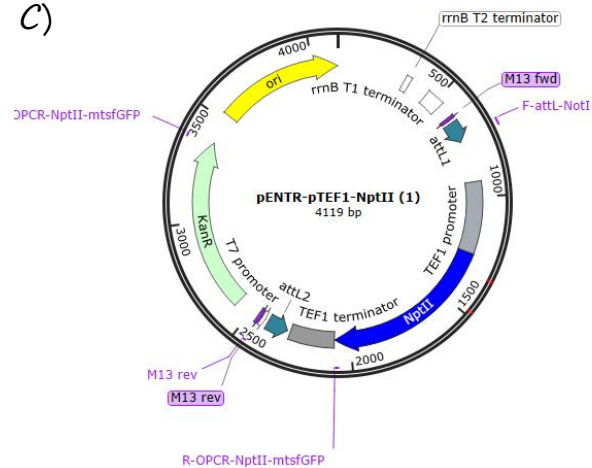


Figure B: The plasmid's map for each DNA template. In part A, this is the template for amplifying *mtNptII*, while part B, the plasmid is amplifying *mtsfGFP*. In part C, the plasmid is used for amplifying the *NptII* gene.

Appendix C

A

ire	Expect	Identities	Gaps	Strand
29 bits(1315)	0.0	1315/1315(100%)	0/1315(0%)	Plus/Plus
Query 1	CGCCCCCTTCACCGGTGATGACGGTGAACCTCTGACACATGCAGCTCCCGGAGACGGT	60		
Sbjct 1	CGCCCCCTTCACCGGTGATGACGGTGAACCTCTGACACATGCAGCTCCCGGAGACGGT	60		
Query 61	CACAGCTTGTCTGTAAGCGGATGCCGGGAGCAGACAAGCCCGTCAGGGCGCGTCAGCGGG	120		
Sbjct 61	CACAGCTTGTCTGTAAGCGGATGCCGGGAGCAGACAAGCCCGTCAGGGCGCGTCAGCGGG	120		
Query 121	TGTTGGCGGGTGTCTGGGGCTGGCTTAACCTATGCGGCATCAGAGCAGATTGTAAGAGT	180		
Sbjct 121	TGTTGGCGGGTGTCTGGGGCTGGCTTAACCTATGCGGCATCAGAGCAGATTGTAAGAGT	180		
Query 181	GCACCATACCAAGGCCAGAAATACCTCCTTGACAGTCTTGACGTGCGCAGCTCAGGGGC	240		
Sbjct 181	GCACCATACCAAGGCCAGAAATACCTCCTTGACAGTCTTGACGTGCGCAGCTCAGGGGC	240		
Query 241	ATGATGTGACTGTGCGCCGTACATTTAGCCCATACATCCCATGTATAATCATTTGCATC	300		
Sbjct 241	ATGATGTGACTGTGCGCCGTACATTTAGCCCATACATCCCATGTATAATCATTTGCATC	300		
Query 301	CATACATTTTGTATGGCCGACGGCGCAAGCAAAAATTACGGCTCCTCGCTGCAGACCTG	360		
Sbjct 301	CATACATTTTGTATGGCCGACGGCGCAAGCAAAAATTACGGCTCCTCGCTGCAGACCTG	360		
Query 361	CGAGCAGGGAAACGCTCCCTCACAGACGCGTTGAATTGTCCCACGCCGCGCCCTGTA	420		
Sbjct 361	CGAGCAGGGAAACGCTCCCTCACAGACGCGTTGAATTGTCCCACGCCGCGCCCTGTA	420		
Query 421	GAGAAATATAAAGGTTAGGATTTGCCACTGAGGTTCTTCTTTTATATACTTCTTTTAA	480		
Sbjct 421	GAGAAATATAAAGGTTAGGATTTGCCACTGAGGTTCTTCTTTTATATACTTCTTTTAA	480		
Query 481	AATCTTGCTAGGATACAGTTCTCACATCACATCCGAACATAAACAACCATGGGTAAGGAA	540		
Sbjct 481	AATCTTGCTAGGATACAGTTCTCACATCACATCCGAACATAAACAACCATGGGTAAGGAA	540		
Query 541	AAGACTCACGTTTCGAGGCCGCGATTAAATTCACATGGATGCTGATTTATATGGGTAT	600		
Sbjct 541	AAGACTCACGTTTCGAGGCCGCGATTAAATTCACATGGATGCTGATTTATATGGGTAT	600		
Query 601	AAATGGGCTCGCGATAATGTCGGGCAATCAGGTGCGACAATCTATCGATTGTATGGGAAG	660		
Sbjct 601	AAATGGGCTCGCGATAATGTCGGGCAATCAGGTGCGACAATCTATCGATTGTATGGGAAG	660		
Query 661	CCCGATGCGCCAGAGTTGTTTCTGAAACATGGCAAAGGTAGCGTTGCCAATGATGTTACA	720		
Sbjct 661	CCCGATGCGCCAGAGTTGTTTCTGAAACATGGCAAAGGTAGCGTTGCCAATGATGTTACA	720		
Query 721	GATGAGATGGTCAGACTAACTGGCTGACGGAATTTATGCCTCTTCCGACCATCAAGCAT	780		
Sbjct 721	GATGAGATGGTCAGACTAACTGGCTGACGGAATTTATGCCTCTTCCGACCATCAAGCAT	780		
Query 781	TTTATCCGTACTCCTGATGATGCATGGTTACTCACCCTGCGATCCCCGGCAAACAGCA	840		
Sbjct 781	TTTATCCGTACTCCTGATGATGCATGGTTACTCACCCTGCGATCCCCGGCAAACAGCA	840		
Query 841	TTCCAGGTATTAGAAGAATATCCTGATTGAGGTGAAAATATTGTTGATGCGCTGGCAGTG	900		
Sbjct 841	TTCCAGGTATTAGAAGAATATCCTGATTGAGGTGAAAATATTGTTGATGCGCTGGCAGTG	900		
Query 901	TTCTGCGCCGGTTGCATTGATTCTGTTTGTAAATTGTCTTTTAAACAGCATCGCGTA	960		
Sbjct 901	TTCTGCGCCGGTTGCATTGATTCTGTTTGTAAATTGTCTTTTAAACAGCATCGCGTA	960		
Query 961	TTTCGTCTCGCTCAGGCGCAATCACGAATGAATAACGGTTTGGTTGATGCGAGTGATTTT	1020		
Sbjct 961	TTTCGTCTCGCTCAGGCGCAATCACGAATGAATAACGGTTTGGTTGATGCGAGTGATTTT	1020		
Query 1021	GATGACGAGCGTAATGGCTGGCTGTTGAACAAGTCTGGAAAGAAATGCATAAGCTTTTG	1080		
Sbjct 1021	GATGACGAGCGTAATGGCTGGCTGTTGAACAAGTCTGGAAAGAAATGCATAAGCTTTTG	1080		

Query	1021	GATGACGAGCGTAATGGCTGGCCTGTTGAACAAGTCTGGAAAGAAATGCATAAGCTTTTG	1080
Sbjct	1021	GATGACGAGCGTAATGGCTGGCCTGTTGAACAAGTCTGGAAAGAAATGCATAAGCTTTTG	1080
Query	1081	CCATTCTACCGGATTCAAGTCGTCATCATGGTGATTTCTCACTTGATAACCTTATTTTT	1140
Sbjct	1081	CCATTCTACCGGATTCAAGTCGTCATCATGGTGATTTCTCACTTGATAACCTTATTTTT	1140
Query	1141	GACGAGGGGAAATTAATAGGTTGTATTGATGTTGGACGAGTCGGAATCGCAGACCGATAC	1200
Sbjct	1141	GACGAGGGGAAATTAATAGGTTGTATTGATGTTGGACGAGTCGGAATCGCAGACCGATAC	1200
Query	1201	CAGGATCTTGCCATCCTATGGAAGTCCTCGGTGAGTTTTCTCCTTCATTACAGAAACGG	1260
Sbjct	1201	CAGGATCTTGCCATCCTATGGAAGTCCTCGGTGAGTTTTCTCCTTCATTACAGAAACGG	1260
Query	1261	CTTTTTCAAAAATATGGTATTGATAATCCTGATATGAATAAATTGCAGTTTCATT	1315
Sbjct	1261	CTTTTTCAAAAATATGGTATTGATAATCCTGATATGAATAAATTGCAGTTTCATT	1315

B)

Score	Expect	Identities	Gaps	Strand
1389 bits(752)	0.0	752/752(100%)	0/752(0%)	Plus/Plus
Query 1	AAGGTGAAGAATTATTCAC	GGTGGTGTGTACCAATTTT	AGTTGAATTAGATGGT	GATGTTA 60
Sbjct 1	AAGGTGAAGAATTATTCAC	GGTGGTGTGTACCAATTTT	AGTTGAATTAGATGGT	GATGTTA 60
Query 61	ATGGTCATAAATTTTCTGT	AAGAGGTGAAGGTGAAGGT	GATGCTACAAACGGAAA	ATTAA 120
Sbjct 61	ATGGTCATAAATTTTCTGT	AAGAGGTGAAGGTGAAGGT	GATGCTACAAACGGAAA	ATTAA 120
Query 121	CTTTAAATTTTATTTGTAC	TACTACTGGAAAATTACCT	GTTCCATGACCAACATT	AGTAACTA 180
Sbjct 121	CTTTAAATTTTATTTGTAC	TACTACTGGAAAATTACCT	GTTCCATGACCAACATT	AGTAACTA 180
Query 181	CTTTAACTTATGGTGTTC	AATGTTTTTCAAGATATCC	AGATCATATGAAAAGAC	ATGATT 240
Sbjct 181	CTTTAACTTATGGTGTTC	AATGTTTTTCAAGATATCC	AGATCATATGAAAAGAC	ATGATT 240
Query 241	TTTTCAAGAGTGCTATGC	CTGAAGGTTATGTTCAAG	AAAGAACATTTTCATT	CAAAGATG 300
Sbjct 241	TTTTCAAGAGTGCTATGC	CTGAAGGTTATGTTCAAG	AAAGAACATTTTCATT	CAAAGATG 300
Query 301	ATGGTACTTACAAGACTA	GAGCTGAAGTAAAGTTT	GAAAGTGATACTTTAG	TTAATAGAA 360
Sbjct 301	ATGGTACTTACAAGACTA	GAGCTGAAGTAAAGTTT	GAAAGTGATACTTTAG	TTAATAGAA 360
Query 361	TCGAATTAAGGTATTGAT	TTTAAAGAAGATGGAA	ACATTTTAGGACATAA	ATTAGAAT 420
Sbjct 361	TCGAATTAAGGTATTGAT	TTTAAAGAAGATGGAA	ACATTTTAGGACATAA	ATTAGAAT 420
Query 421	ACAACTTTAACTCACATA	ATGTTTATATTACAGC	AGATAAACAAAAGAAT	GGAATCAAAG 480
Sbjct 421	ACAACTTTAACTCACATA	ATGTTTATATTACAGC	AGATAAACAAAAGAAT	GGAATCAAAG 480
Query 481	CTAACTTCAAAATTAGAC	ATAACGTAGAAGATGG	TCTGTTCAATTAGCAG	ATCATTATC 540
Sbjct 481	CTAACTTCAAAATTAGAC	ATAACGTAGAAGATGG	TCTGTTCAATTAGCAG	ATCATTATC 540
Query 541	AACAAAATACTCCTATT	GGTGATGGTCCTGTAT	TATTACCAGATAACC	ATTACTTATCTA 600
Sbjct 541	AACAAAATACTCCTATT	GGTGATGGTCCTGTAT	TATTACCAGATAACC	ATTACTTATCTA 600
Query 601	CACAATCTGTATTATCT	AAGATCCTAACGAAA	AGAGATCATATGGT	ATTATTAGAAT 660
Sbjct 601	CACAATCTGTATTATCT	AAGATCCTAACGAAA	AGAGATCATATGGT	ATTATTAGAAT 660
Query 661	TTGTAAGTCTGCTGGT	TATTACACATGGTAT	GGATGAATTATACAA	ATAGTCCTAGCATA 720
Sbjct 661	TTGTAAGTCTGCTGGT	TATTACACATGGTAT	GGATGAATTATACAA	ATAGTCCTAGCATA 720
Query 721	ACCCCTTGGGGCCTCT	AACGGGCTTTGAGGG	752	
Sbjct 721	ACCCCTTGGGGCCTCT	AACGGGCTTTGAGGG	752	

Figure C: Alignment of *NptII*-*mtsfGFP* fusion gene product. Part A was *NptII* gene, part B was *mtsfGFP* gene.

Appendix D

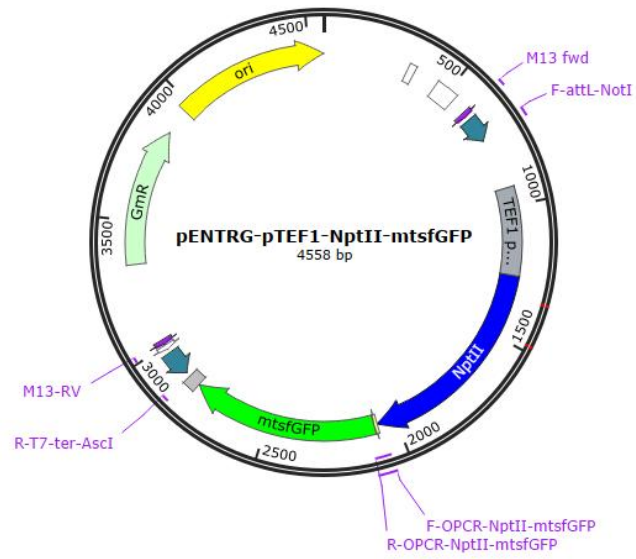


Figure D: Genetic map for *NptII*-*mtsGFP* fusion gene product. The fusion gene product had been successful clone inside *E. coli*.

Appendix E

Score	Expect	Identities	Gaps	Strand
3989 bits(2160)	0.0	2160/2160(100%)	0/2160(0%)	Plus/Plus
Query 1	CAACTTTGTACAAAAAGCAGGCTCCGCGGCCGCCCTTCACCGGTGATGACGGTGAAA			60
Sbjct 1	CAACTTTGTACAAAAAGCAGGCTCCGCGGCCGCCCTTCACCGGTGATGACGGTGAAA			60
Query 61	ACCTCTGACACATGCAGCTCCCGGAGACGGTCACAGCTTGTCTGTAAGCGGATGCCGGGA			120
Sbjct 61	ACCTCTGACACATGCAGCTCCCGGAGACGGTCACAGCTTGTCTGTAAGCGGATGCCGGGA			120
Query 121	GCAGACAAGCCCGTCAGGGCGCGTCAGCGGGTGTGGCGGGTGTGGGGCTGGCTTAACT			180
Sbjct 121	GCAGACAAGCCCGTCAGGGCGCGTCAGCGGGTGTGGCGGGTGTGGGGCTGGCTTAACT			180
Query 181	ATGCGGCATCAGAGCAGATTGTACTGAGAGTGACCATACCAAGGCCAGAAATACCTCC			240
Sbjct 181	ATGCGGCATCAGAGCAGATTGTACTGAGAGTGACCATACCAAGGCCAGAAATACCTCC			240
Query 241	TTGACAGTCTTGACGTGCGCAGCTCAGGGGCATGATGTGACTGTGCGCCGTACATTTAGC			300
Sbjct 241	TTGACAGTCTTGACGTGCGCAGCTCAGGGGCATGATGTGACTGTGCGCCGTACATTTAGC			300
Query 301	CCATACATCCCCATGTATAATCATTTGCATCCATACATTTTGATGGCCGCACGGCGCGAA			360
Sbjct 301	CCATACATCCCCATGTATAATCATTTGCATCCATACATTTTGATGGCCGCACGGCGCGAA			360
Query 361	GCAAAAATTACGGCTCCTCGCTGCAGACCTGCGAGCAGGGAACGCTCCCTCACAGACG			420
Sbjct 361	GCAAAAATTACGGCTCCTCGCTGCAGACCTGCGAGCAGGGAACGCTCCCTCACAGACG			420
Query 421	CGTTGAATTGTCCCGACGCCGCGCCCTGTAGAGAAATATAAAGGTTAGGATTTGCCAC			480
Sbjct 421	CGTTGAATTGTCCCGACGCCGCGCCCTGTAGAGAAATATAAAGGTTAGGATTTGCCAC			480
Query 481	TGAGGTTCTTCTTTTATATACTTCTTTTAAAACTTGTAGGATACAGTTCTCACATCA			540
Sbjct 481	TGAGGTTCTTCTTTTATATACTTCTTTTAAAACTTGTAGGATACAGTTCTCACATCA			540
Query 541	CATCCGAACATAAACCAACCATGGGTAAAGGAAAAGACTCACGTTTCGAGGCCGCGATTA			600
Sbjct 541	CATCCGAACATAAACCAACCATGGGTAAAGGAAAAGACTCACGTTTCGAGGCCGCGATTA			600
Query 601	TTCCAACATGGATGCTGATTATATGGGTATAAATGGGCTCGCGATAATGTCGGGCAATC			660
Sbjct 601	TTCCAACATGGATGCTGATTATATGGGTATAAATGGGCTCGCGATAATGTCGGGCAATC			660
Query 661	AGGTGCGACAATCTATCGATTGTATGGGAAGCCGATGCGCCAGAGTTGTTTCTGAAACA			720
Sbjct 661	AGGTGCGACAATCTATCGATTGTATGGGAAGCCGATGCGCCAGAGTTGTTTCTGAAACA			720
Query 721	TGGCAAAGGTAGCGTTGCCAATGATGTTACAGATGAGATGGTCAGACTAACTGGCTGAC			780
Sbjct 721	TGGCAAAGGTAGCGTTGCCAATGATGTTACAGATGAGATGGTCAGACTAACTGGCTGAC			780
Query 781	GGAATTTATGCCTCTTCCGACCATCAAGCATTTTATCCGTAATCCTGATGATGCATGGTT			840
Sbjct 781	GGAATTTATGCCTCTTCCGACCATCAAGCATTTTATCCGTAATCCTGATGATGCATGGTT			840
Query 841	ACTCACCAGTGCATCCCCGGCAAAACAGCATTCCAGGTATTAGAAGAATATCCTGATTC			900
Sbjct 841	ACTCACCAGTGCATCCCCGGCAAAACAGCATTCCAGGTATTAGAAGAATATCCTGATTC			900
Query 901	AGGTGAAAATATTGTTGATGCGCTGGCAGTGTTCTGCGCCGGTTGCATTTCGATTCTGT			960
Sbjct 901	AGGTGAAAATATTGTTGATGCGCTGGCAGTGTTCTGCGCCGGTTGCATTTCGATTCTGT			960
Query 961	TTGTAATTGTCCTTTTAAACAGCGATCGCGTATTTTCGTCTCGCTCAGGCGCAATCACGA			1020
Sbjct 961	TTGTAATTGTCCTTTTAAACAGCGATCGCGTATTTTCGTCTCGCTCAGGCGCAATCACGA			1020

Query	1021	GAATAACGGTTTGGTTGATGCGAGTGATTTTGATGACGAGCGTAATGGCTGGCCTGTTGA	1080
Sbjct	1021	GAATAACGGTTTGGTTGATGCGAGTGATTTTGATGACGAGCGTAATGGCTGGCCTGTTGA	1080
Query	1081	ACAAGTCTGGAAAGAAATGCATAAGCTTTTGCCATTCTCACCAGGATTAGTCGTCACCTCA	1140
Sbjct	1081	ACAAGTCTGGAAAGAAATGCATAAGCTTTTGCCATTCTCACCAGGATTAGTCGTCACCTCA	1140
Query	1141	TGGTGATTTCTCACTTGATAACCTTATTTTGGACGAGGGGAAATTAATAGGTTGTATTGA	1200
Sbjct	1141	TGGTGATTTCTCACTTGATAACCTTATTTTGGACGAGGGGAAATTAATAGGTTGTATTGA	1200
Query	1201	TGTTGGACGAGTCGGAATCGCAGACCGATACCAGGATCTTGCCATCCTATGGAACGCT	1260
Sbjct	1201	TGTTGGACGAGTCGGAATCGCAGACCGATACCAGGATCTTGCCATCCTATGGAACGCT	1260
Query	1261	CGGTGAGTTTTCTCCTTCATTACAGAAACGGCTTTTTCAAAAATATGGTATTGATAATCC	1320
Sbjct	1261	CGGTGAGTTTTCTCCTTCATTACAGAAACGGCTTTTTCAAAAATATGGTATTGATAATCC	1320
Query	1321	TGATATGAATAAAATTCAGTTCATTGATGCTCGATGAGTTTTTCGGATCCGAGACCAT	1380
Sbjct	1321	TGATATGAATAAAATTCAGTTCATTGATGCTCGATGAGTTTTTCGGATCCGAGACCAT	1380
Query	1381	GTCTAAAGGTGAAGAATTATTCAGTGGTGTGTACCAATTTTAGTTGAATTAGATGGTGA	1440
Sbjct	1381	GTCTAAAGGTGAAGAATTATTCAGTGGTGTGTACCAATTTTAGTTGAATTAGATGGTGA	1440
Query	1441	TGTTAATGGTCATAAAATTTCTGTAAGAGGTGAAGGTGAAGGTGATGCTACAAACGGAAA	1500
Sbjct	1441	TGTTAATGGTCATAAAATTTCTGTAAGAGGTGAAGGTGAAGGTGATGCTACAAACGGAAA	1500
Query	1501	ATTAACCTTTAAAATTTATTTGTACTACTGGAAAATTACCTGTTCCATGACCAACATTAGT	1560
Sbjct	1501	ATTAACCTTTAAAATTTATTTGTACTACTGGAAAATTACCTGTTCCATGACCAACATTAGT	1560
Query	1021	GAATAACGGTTTGGTTGATGCGAGTGATTTTGATGACGAGCGTAATGGCTGGCCTGTTGA	1080
Sbjct	1021	GAATAACGGTTTGGTTGATGCGAGTGATTTTGATGACGAGCGTAATGGCTGGCCTGTTGA	1080
Query	1081	ACAAGTCTGGAAAGAAATGCATAAGCTTTTGCCATTCTCACCAGGATTAGTCGTCACCTCA	1140
Sbjct	1081	ACAAGTCTGGAAAGAAATGCATAAGCTTTTGCCATTCTCACCAGGATTAGTCGTCACCTCA	1140
Query	1141	TGGTGATTTCTCACTTGATAACCTTATTTTGGACGAGGGGAAATTAATAGGTTGTATTGA	1200
Sbjct	1141	TGGTGATTTCTCACTTGATAACCTTATTTTGGACGAGGGGAAATTAATAGGTTGTATTGA	1200
Query	1201	TGTTGGACGAGTCGGAATCGCAGACCGATACCAGGATCTTGCCATCCTATGGAACGCT	1260
Sbjct	1201	TGTTGGACGAGTCGGAATCGCAGACCGATACCAGGATCTTGCCATCCTATGGAACGCT	1260
Query	1261	CGGTGAGTTTTCTCCTTCATTACAGAAACGGCTTTTTCAAAAATATGGTATTGATAATCC	1320
Sbjct	1261	CGGTGAGTTTTCTCCTTCATTACAGAAACGGCTTTTTCAAAAATATGGTATTGATAATCC	1320
Query	1321	TGATATGAATAAAATTCAGTTCATTGATGCTCGATGAGTTTTTCGGATCCGAGACCAT	1380
Sbjct	1321	TGATATGAATAAAATTCAGTTCATTGATGCTCGATGAGTTTTTCGGATCCGAGACCAT	1380
Query	1381	GTCTAAAGGTGAAGAATTATTCAGTGGTGTGTACCAATTTTAGTTGAATTAGATGGTGA	1440
Sbjct	1381	GTCTAAAGGTGAAGAATTATTCAGTGGTGTGTACCAATTTTAGTTGAATTAGATGGTGA	1440
Query	1441	TGTTAATGGTCATAAAATTTCTGTAAGAGGTGAAGGTGAAGGTGATGCTACAAACGGAAA	1500
Sbjct	1441	TGTTAATGGTCATAAAATTTCTGTAAGAGGTGAAGGTGAAGGTGATGCTACAAACGGAAA	1500
Query	1501	ATTAACCTTTAAAATTTATTTGTACTACTGGAAAATTACCTGTTCCATGACCAACATTAGT	1560
Sbjct	1501	ATTAACCTTTAAAATTTATTTGTACTACTGGAAAATTACCTGTTCCATGACCAACATTAGT	1560

Query	1561	AACTACTTTAACTTATGGTGTTCAATGTTTTCAAGATATCCAGATCATATGAAAAGACA	1620
Sbjct	1561	AACTACTTTAACTTATGGTGTTCAATGTTTTCAAGATATCCAGATCATATGAAAAGACA	1620
Query	1621	TGATTTTTTCAAGAGTGCTATGCCTGAAGGTTATGTTCAAGAAAGAACAATTTCAATTCAA	1680
Sbjct	1621	TGATTTTTTCAAGAGTGCTATGCCTGAAGGTTATGTTCAAGAAAGAACAATTTCAATTCAA	1680
Query	1681	AGATGATGGTACTTACAAGACTAGAGCTGAAGTAAAGTTTGAAGGTGATACTTTAGTTAA	1740
Sbjct	1681	AGATGATGGTACTTACAAGACTAGAGCTGAAGTAAAGTTTGAAGGTGATACTTTAGTTAA	1740
Query	1741	TAGAATCGAATTAAGGTTATGATTTTAAAGAAGATGGAACATTTTAGGACATAAATT	1800
Sbjct	1741	TAGAATCGAATTAAGGTTATGATTTTAAAGAAGATGGAACATTTTAGGACATAAATT	1800
Query	1801	AGAATACAACTTAACTCACATAATGTTTATATTACAGCAGATAAACAAGAAATGGAAT	1860
Sbjct	1801	AGAATACAACTTAACTCACATAATGTTTATATTACAGCAGATAAACAAGAAATGGAAT	1860
Query	1861	CAAAGCTAACTTCAAAATTAGACATAACGTAGAAGATGGTCTGTTCAATTAGCAGATCA	1920
Sbjct	1861	CAAAGCTAACTTCAAAATTAGACATAACGTAGAAGATGGTCTGTTCAATTAGCAGATCA	1920
Query	1921	TTATCAACAAAATACTCCTATTGGTGATGGTCCTGTATTATTACCAGATAACCATTACTT	1980
Sbjct	1921	TTATCAACAAAATACTCCTATTGGTGATGGTCCTGTATTATTACCAGATAACCATTACTT	1980
Query	1981	ATCTACACAATCTGTATTATCTAAAGATCCTAACGAAAAGAGAGATCATATGGTATTATT	2040
Sbjct	1981	ATCTACACAATCTGTATTATCTAAAGATCCTAACGAAAAGAGAGATCATATGGTATTATT	2040
Query	2041	AGAATTTGTAAGTGTGCTGGTATTACACATGGTATGGATGAATTATACAAATAGTCCTA	2100
Sbjct	2041	AGAATTTGTAAGTGTGCTGGTATTACACATGGTATGGATGAATTATACAAATAGTCCTA	2100
Query	2101	GCATAACCCCTTGGGGCCTCTAACGGGCTTGAGGGGTTTTTTGAAGGGTGGGCGCGCC	2160
Sbjct	2101	GCATAACCCCTTGGGGCCTCTAACGGGCTTGAGGGGTTTTTTGAAGGGTGGGCGCGCC	2160

Figure E: Alignment of *NptII*^{-mt}*sfGFP* fusion gene product.

Appendix F

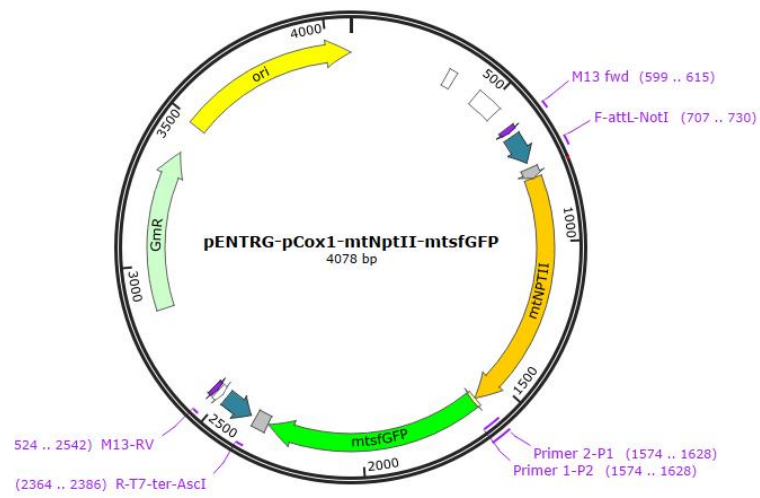


Figure F: Genetic map for *mtNptII*-*mtsfgfp* fusion gene product. The fusion gene product had been successful clone inside *E. coli*.

Appendix G

Score	Expect	Identities	Gaps	Strand
3103 bits(1680)	0.0	1680/1680(100%)	0/1680(0%)	Plus/Plus
Query 1	CAACTTTGTACAAAAAGCAGGCTCCGCGGCCGCCCTTCACCGTATTGATATAAGTAA	60		
Sbjct 1	CAACTTTGTACAAAAAGCAGGCTCCGCGGCCGCCCTTCACCGTATTGATATAAGTAA	60		
Query 61	TAGATATAATAATAATATTATGGGTAAGGAAAAGACTCACGTTTCTCGTCCTCGTTTAAA	120		
Sbjct 61	TAGATATAATAATAATATTATGGGTAAGGAAAAGACTCACGTTTCTCGTCCTCGTTTAAA	120		
Query 121	TTCTAATATGGATGCTGATTTATATGGTTATAAGTGAGCTCGTGATAATGTTGGTCAATC	180		
Sbjct 121	TTCTAATATGGATGCTGATTTATATGGTTATAAGTGAGCTCGTGATAATGTTGGTCAATC	180		
Query 181	TGGTGCTACTATTTATCGTTTATATGGTAAGCCTGACGCTCCTGAATTGTTTTGAAGCA	240		
Sbjct 181	TGGTGCTACTATTTATCGTTTATATGGTAAGCCTGACGCTCCTGAATTGTTTTGAAGCA	240		
Query 241	TGGTAAAGGTTCTGTTGCTAATGATGTTACTGATGAAATGGTCCGTTTAAATTGATTAAC	300		
Sbjct 241	TGGTAAAGGTTCTGTTGCTAATGATGTTACTGATGAAATGGTCCGTTTAAATTGATTAAC	300		
Query 301	TGAATTTATGCCTTTACCTACTATTAAACATTTTATTCGTA CTCTGATGATGCTTGATT	360		
Sbjct 301	TGAATTTATGCCTTTACCTACTATTAAACATTTTATTCGTA CTCTGATGATGCTTGATT	360		
Query 361	GTTAACTACTGCTATTCTGGTAAGACTGCTTTTCAAGTCTTAGAAGAATATCCTGATTC	420		
Sbjct 361	GTTAACTACTGCTATTCTGGTAAGACTGCTTTTCAAGTCTTAGAAGAATATCCTGATTC	420		
Query 421	TGGTGAAAATATTGTTGATGCTTTAGCTGTCTTTTACGTCGTTTACATTCTATTCTCTGT	480		
Sbjct 421	TGGTGAAAATATTGTTGATGCTTTAGCTGTCTTTTACGTCGTTTACATTCTATTCTCTGT	480		
Query 481	TTGTAATTGTCCTTTAATTCTGATCGTGTTTTTCGTTTAGCTCAAGCTCAATCTCGTAT	540		
Sbjct 481	TTGTAATTGTCCTTTAATTCTGATCGTGTTTTTCGTTTAGCTCAAGCTCAATCTCGTAT	540		
Query 541	GAACAATGGTTTAGTTGATGCTTCTGATTTTCGACGATGACCGTAACGGTTGACCTGTTGA	600		
Sbjct 541	GAACAATGGTTTAGTTGATGCTTCTGATTTTCGACGATGACCGTAACGGTTGACCTGTTGA	600		
Query 601	ACAAGTTTGAAAGGAAATGCATAAGTTATTACCTTTTCTCCTGATTCTGTTGTTACTCA	660		
Sbjct 601	ACAAGTTTGAAAGGAAATGCATAAGTTATTACCTTTTCTCCTGATTCTGTTGTTACTCA	660		
Query 661	TGGTGACTTCTCTTTAGACAATTTAATTTTCGATGAAGGTAAGTTGATCGGTTGTATCGA	720		
Sbjct 661	TGGTGACTTCTCTTTAGACAATTTAATTTTCGATGAAGGTAAGTTGATCGGTTGTATCGA	720		
Query 721	TGTCGGTCGTGTCGGTATCGTGACCGTTACCAAGACTTGGCTATCTTGTGAAACTGTTT	780		
Sbjct 721	TGTCGGTCGTGTCGGTATCGTGACCGTTACCAAGACTTGGCTATCTTGTGAAACTGTTT	780		
Query 781	AGGTGAGTTCTCTCTTCCCTTGACAGGCGTTTGTTCAAAAGTATGGTATCGATAACCC	840		
Sbjct 781	AGGTGAGTTCTCTCTTCCCTTGACAGGCGTTTGTTCAAAAGTATGGTATCGATAACCC	840		
Query 841	TGACATGAATAAATTACAGTTCCACTTGATGTTGGACGAGTTCTTCGGATCCGAGACCAT	900		
Sbjct 841	TGACATGAATAAATTACAGTTCCACTTGATGTTGGACGAGTTCTTCGGATCCGAGACCAT	900		
Query 901	GTCTAAAGGTGAAGAATTATTCAGTGGTGTGTACCAATTTTAGTTGAATTAGATGGTGA	960		
Sbjct 901	GTCTAAAGGTGAAGAATTATTCAGTGGTGTGTACCAATTTTAGTTGAATTAGATGGTGA	960		
Query 961	TGTTAATGGTCATAAAATTTCTGTAAAGAGGTGAAGGTGAAGGTGATGCTACAAACGAAA	1020		
Sbjct 961	TGTTAATGGTCATAAAATTTCTGTAAAGAGGTGAAGGTGAAGGTGATGCTACAAACGAAA	1020		
Query 1021	ATTAACCTTTAAATTTATTTGTACTACTGGAAAATTACCTGTTCCATGACCAACATTAGT	1080		
Sbjct 1021	ATTAACCTTTAAATTTATTTGTACTACTGGAAAATTACCTGTTCCATGACCAACATTAGT	1080		
Query 1081	AACTACTTTAACTTATGGTGTTCAATGTTTTTCAAGATATCCAGATCATATGAAAAGACA	1140		
Sbjct 1081	AACTACTTTAACTTATGGTGTTCAATGTTTTTCAAGATATCCAGATCATATGAAAAGACA	1140		

Query	1141	TGATTTTTTCAAGAGTGCTATGCCTGAAGGTTATGTTCAAGAAAGAACAATTTCAATTCAA	1200
Sbjct	1141	TGATTTTTTCAAGAGTGCTATGCCTGAAGGTTATGTTCAAGAAAGAACAATTTCAATTCAA	1200
Query	1201	AGATGATGGTACTTACAAGACTAGAGCTGAAGTAAAGTTTGAAGGTGATACTTTAGTTAA	1260
Sbjct	1201	AGATGATGGTACTTACAAGACTAGAGCTGAAGTAAAGTTTGAAGGTGATACTTTAGTTAA	1260
Query	1261	TAGAATCGAATTAAGGTTATTGATTTTAAAGAAGATGGAAACATTTTAGGACATAAATT	1320
Sbjct	1261	TAGAATCGAATTAAGGTTATTGATTTTAAAGAAGATGGAAACATTTTAGGACATAAATT	1320
Query	1321	AGAATACAACCTTAACTCACATAATGTTTATATTACAGCAGATAAACAAAAGAATGGAAT	1380
Sbjct	1321	AGAATACAACCTTAACTCACATAATGTTTATATTACAGCAGATAAACAAAAGAATGGAAT	1380
Query	1381	CAAAGCTAACTTCAAAATTAGACATAACGTAGAAGATGGTTCTGTTCAATTAGCAGATCA	1440
Sbjct	1381	CAAAGCTAACTTCAAAATTAGACATAACGTAGAAGATGGTTCTGTTCAATTAGCAGATCA	1440
Query	1441	TTATCAACAAAATACTCCTATTGGTGATGGTCCTGTATTATTACCAGATAACCATTACTT	1500
Sbjct	1441	TTATCAACAAAATACTCCTATTGGTGATGGTCCTGTATTATTACCAGATAACCATTACTT	1500
Query	1501	ATCTACACAATCTGTATTATCTAAAGATCCTAACGAAAAGAGAGATCATATGGTATTATT	1560
Sbjct	1501	ATCTACACAATCTGTATTATCTAAAGATCCTAACGAAAAGAGAGATCATATGGTATTATT	1560
Query	1561	AGAATTTGTAAGTGCTGCTGGTATTACACATGGTATGGATGAATTATACAAATAGTCCTA	1620
Sbjct	1561	AGAATTTGTAAGTGCTGCTGGTATTACACATGGTATGGATGAATTATACAAATAGTCCTA	1620
Query	1621	GCATAACCCCTTGGGGCCTCTAAACGGGTCTTGAGGGGTTTTTTGAAGGGTGGGCGCGCC	1680
Sbjct	1621	GCATAACCCCTTGGGGCCTCTAAACGGGTCTTGAGGGGTTTTTTGAAGGGTGGGCGCGCC	1680

Figure G: Alignment of *NptII*-*sfGFP* fusion gene product.

FACULTY OF SCIENCE
UNIVERSITI TUNKU ABDUL RAHMAN

Date: _____

PERMISSION SHEET

It is hereby certified that CHENG YANG YAN (ID No: 22ADB07553) has completed this final year project report entitled “CONSTRUCTION OF *NptII-miRsfGFP* FUSION GENE CONSTRUCT BY OVERLAP EXTENSION PCR” under the supervision of Prof. Dr. Wong Hann Ling from the Department of Biological Science, Faculty of Science.

I hereby give permission to the University to upload the softcopy of my final year project dissertation in pdf format into the UTAR Institutional Repository, which may be made accessible to the UTAR community and public.

I hereby give permission to my supervisor to write and prepare manuscript of these research findings for publishing in any form, if I did not prepare it within six (6) months’ time from this date provided that my name is included as one of the authors for this article. Arrangement of the name depends on my supervisor.

Yours truly,

(CHENG YANG YAN)



Widely owned by a UNL Graduate Foundation
SINCE 1982

Universiti Tunku Abdul Rahman			
Form Title : Supervisor's Comments on Originality Report Generated by Turnitin for Submission of Final Year Project Report (for Undergraduate Programmes)			
Form Number: FM-IAD-005	Rev No.: 1	Effective Date: 3/10/2019	Page No.: 1 of 1

FACULTY OF SCIENCE

Full Name(s) of Candidate(s)	Chang Yang Yan
ID Number(s)	22ADB07533
Programme / Course	BACHELOR OF SCIENCE (HONOURS) BIOTECHNOLOGY
Title of Final Year Project	CONSTRUCTION OF NptII-mnEGFP FUSION GENE CONSTRUCT BY OVERLAP EXTENSION PCR

Similarity	Supervisor's Comments (Compulsory if parameters of originality exceeds the limits approved by UTAR)
Overall similarity index: <u>14</u>	
% Similarity by source Internet Sources: <u>8</u> % Publications: <u>6</u> % Student Papers: <u>11</u> %	
Number of individual sources listed of more than 3% similarity: <u>0</u>	
Parameters of originality required and limits approved by UTAR are as follows: (i) Overall similarity index is 20% and below, and (ii) Matching of individual sources listed must be less than 3% each, and (iii) Matching texts in continuous block must not exceed 8 words <i>Note: Parameters (i) – (iii) shall exclude quotes, bibliography and text matches which are less than 8 words.</i>	

Note: Supervisor/Candidate(s) is/are required to provide softcopy of full set of the originality report to Faculty/Institute

Based on the above results, I hereby declare that I am satisfied with the originality of the Final Year Project Report submitted by my student(s) as named above.

Signature of Supervisor

Signature of Co-Supervisor

Name: Wong Hann Ling

Name: _____

Date: 03.09.2025

Date: _____

Yang Yan Cheng 

BT-ChengYangYan_FYP Project Report_commented

FYP2025.202

Document Details

Submission ID

36181106234973

Submission Date

Sep 3, 2025, 1:19 AM GMT+8

Download Date

Sep 3, 2025, 2:18 AM GMT+8

File Name

BT-ChengYangYan_FYP Project Report_commented.docx

File Size

1.6 MB

72 Pages

12,224 Words

70,232 Characters

14% Overall Similarity

The combined total of all matches, including overlapping sources, for each database.

Filtered from the Report

▶ Small Matches (less than 8 words)

Match Groups

- 15 Not Cited or Quoted 13%
Matches with neither in-text citation nor quotation marks
- 11 Missing Quotations 1%
Matches that are still very similar to source material
- 0 Missing Citation 0%
Matches that have quotation marks, but no in-text citation
- 0 Cited and Quoted 0%
Matches with in-text citation present, but no quotation marks

Top Sources

- 0% Internet sources
- 0% Publications
- 11% Submitted works (Student Papers)

Integrity Flags

0 Integrity Flags for Review

Our systems algorithm looks deeply at a document for any inconsistencies that would set it apart from a normal submission. If we notice something strange, we flag it for you to review.

A flag is not necessarily an indicator of a problem, however, we'd recommend you focus your attention there for further review.